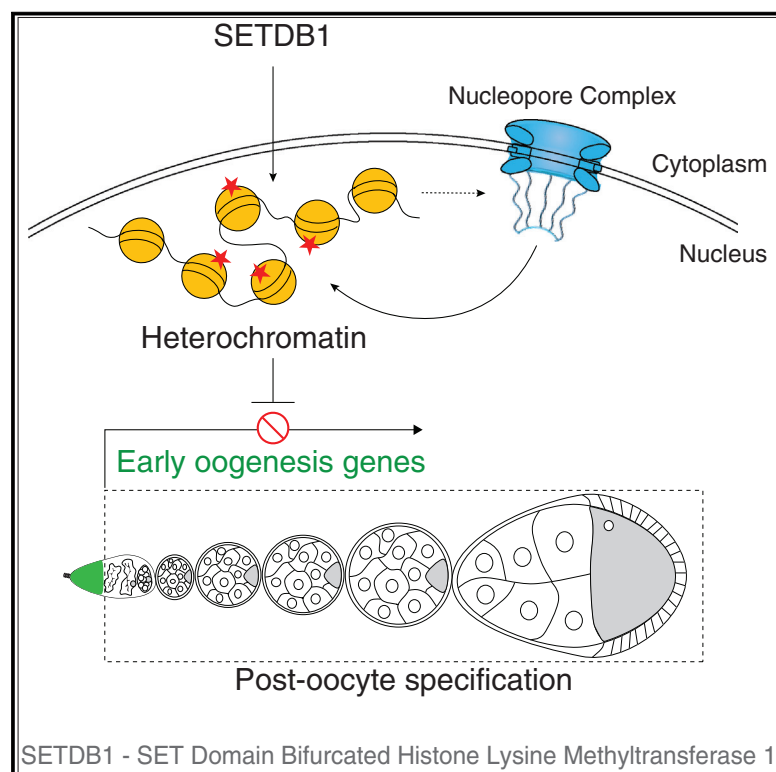


Developmental Cell

A feedback loop between heterochromatin and the nucleopore complex controls germ-cell-to-oocyte transition during *Drosophila* oogenesis

Graphical abstract



Authors

Kahini Sarkar, Noor M. Kotb,
Alex Lemus, ..., Alex M. Valm,
Morgan A. Sammons,
Prashanth Rangan

Correspondence

prashanth.rangan@mssm.edu

In brief

Sarkar et al. describe how a cohort of early-oogenesis genes are silenced by heterochromatin formation during oocyte specification. The heterochromatin promotes nucleopore complex (NPC) formation, which in turn helps maintain silenced genes to developmentally regulate gene silencing and fertility.

Highlights

- H3K9me3 heterochromatin silences early-oogenesis genes during oocyte specification
- H3K9me3 heterochromatin is required for nucleopore complex formation
- Function of NPCs is required for silencing early-oogenesis genes
- Silencing of early-oogenesis genes is essential for the maintenance of oocyte fate

Article

A feedback loop between heterochromatin and the nucleopore complex controls germ-cell-to-oocyte transition during *Drosophila* oogenesis

Kahini Sarkar,¹ Noor M. Kotb,^{1,2} Alex Lemus,¹ Elliot T. Martin,¹ Alicia McCarthy,^{1,3} Justin Camacho,¹ Ayman Iqbal,¹ Alex M. Valm,¹ Morgan A. Sammons,¹ and Prashanth Rangan^{1,4,*}

¹Department of Biological Sciences and RNA Institute, University at Albany SUNY, Albany, NY 12222, USA

²Department of Biomedical Sciences, School of Public Health, University at Albany SUNY, Albany, NY 12222, USA

³Present address: 10x Genomics Headquarters, 6230 Stoneridge Mall Rd, Pleasanton, CA 94588, USA

⁴Lead contact

*Correspondence: prashanth.rangan@mssm.edu

<https://doi.org/10.1016/j.devcel.2023.08.014>

SUMMARY

Germ cells differentiate into oocytes that launch the next generation upon fertilization. How the highly specialized oocyte acquires this distinct cell fate is poorly understood. During *Drosophila* oogenesis, H3K9me3 histone methyltransferase SETDB1 translocates from the cytoplasm to the nucleus of germ cells concurrently with oocyte specification. Here, we discovered that nuclear SETDB1 is required for silencing a cohort of differentiation-promoting genes by mediating their heterochromatinization. Intriguingly, SETDB1 is also required for upregulating 18 of the ~30 nucleoporins (Nups) that compose the nucleopore complex (NPC), promoting NPC formation. NPCs anchor SETDB1-dependent heterochromatin at the nuclear periphery to maintain H3K9me3 and gene silencing in the egg chambers. Aberrant gene expression due to the loss of SETDB1 or Nups results in the loss of oocyte identity, cell death, and sterility. Thus, a feedback loop between heterochromatin and NPCs promotes transcriptional reprogramming at the onset of oocyte specification, which is critical for establishing oocyte identity.

INTRODUCTION

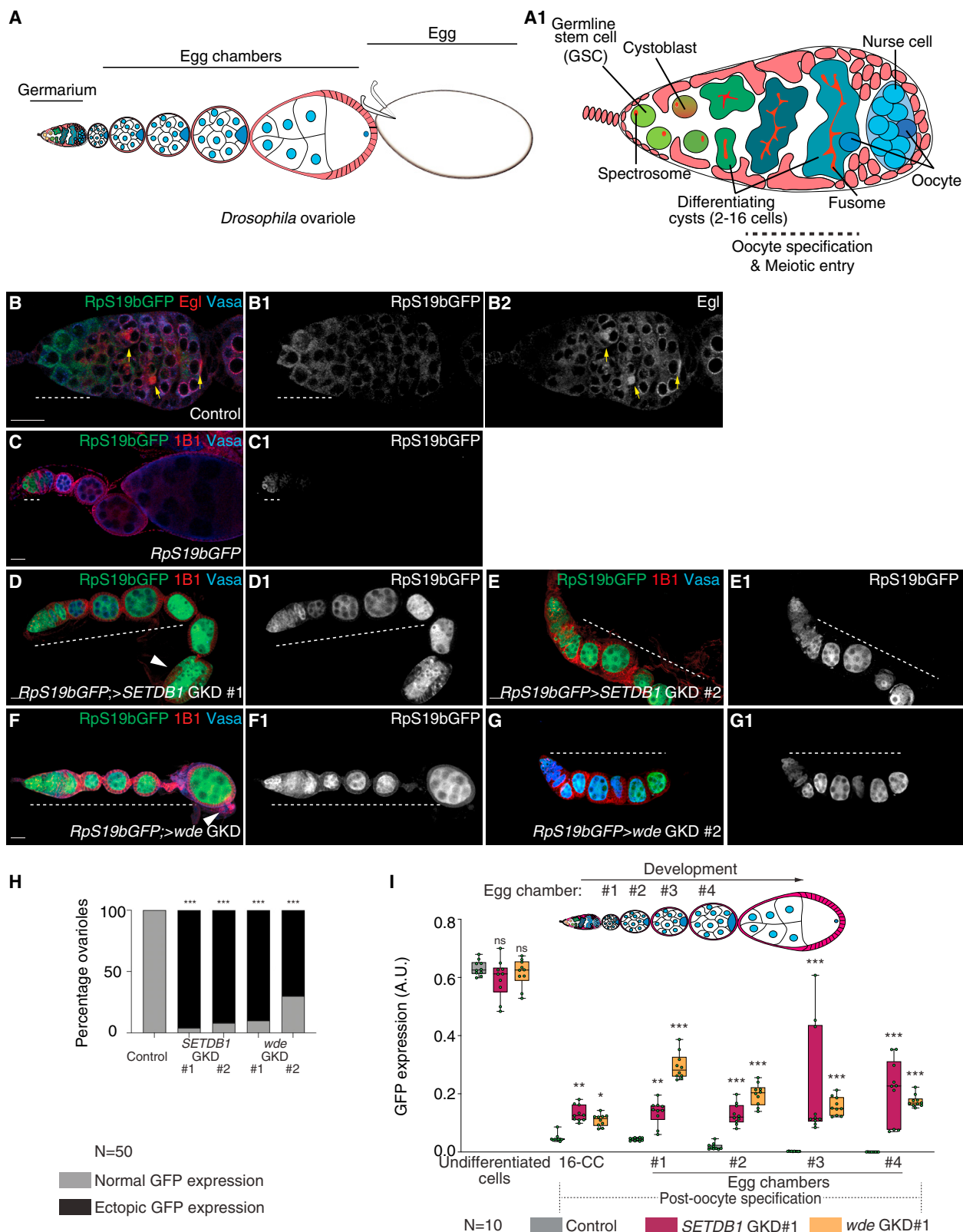
Germ cells give rise to gametes that launch the next generation upon fertilization.^{1–3} Germ cells can become germline stem cells (GSCs) that self-renew and differentiate to give rise to sperm or an oocyte.^{1,4–6} Upon fertilization, the oocyte can differentiate into every cell lineage in the adult organism.^{7,8} The gene regulatory mechanisms that enable the transition from germ cells to oocytes are not fully understood.

Drosophila has a well-characterized transition from a GSC to an oocyte.^{2,4} *Drosophila* ovaries comprise individual units called ovarioles that house the GSCs in the germarium (Figures 1A and 1A1).^{7,9} GSC division results in a new GSC and a cystoblast, which differentiates via incomplete mitotic divisions, giving rise to 2-, 4-, 8-, and 16-cell cysts (Figure 1A1).^{10–12} One of these 16 cells is specified as the oocyte, whereas the other 15 cells become nurse cells.^{13,14} Somatic cells envelop the nurse cells and the specified oocyte to form an egg chamber (Figure 1A1).⁹ The nurse cells produce maternal mRNAs, whose deposition into the specified oocyte is mediated by an RNA-binding protein, Egalitarian (Egl).^{14,15} An inability to specify or maintain the oocyte fate leads to death of the egg chamber during oogenesis, resulting in sterility.^{14,16}

The transition from a GSC to an oocyte requires dynamic changes in gene expression.¹⁷ Once a GSC gives rise to the cys-

toblast, it expresses the differentiation factor Bag of marbles (Bam), promoting its differentiation to an 8-cell cyst.^{18,19} In the 8-cell cyst, the expression of the RNA binding fox-1 homolog 1 (Rbfox1) is required for mediating the transition into the 16-cell cyst stage, allowing for an oocyte to be specified.²⁰ The translation of Rbfox1 requires increased levels of ribosomal small subunit protein 19 (RpS19), accomplished in part by expression of the germline-specific paralog RpS19b in the undifferentiated and early differentiating stages.^{21,22} During differentiation, the germ line also initiates meiotic recombination, mediated by the synaptonemal complex, which consists of proteins such as Sisters Unbound (Sunn), Corona (Cona), and Orientation Disruptor (Ord).^{23–25} More than one cell in the cyst stage initiates recombination, but as oocyte differentiation proceeds, only the specified oocyte retains the synaptonemal complex (Figure 1A1).^{23,26,27} After oocyte specification, the levels of mRNAs encoding RpS19b and some synaptonemal complex proteins are diminished, suggesting that early-oogenesis genes are no longer expressed.²² How the expression of these early-oogenesis genes is attenuated is not known.

In *Drosophila*, the SET domain bifurcated histone lysine methyltransferase 1 (SETDB1) (also called Eggless) is required for the deposition of gene silencing histone H3 lysine 9 trimethylation (H3K9me3) marks and heterochromatin formation.^{28–30}



(legend on next page)

Developmental Cell

Article



SETDB1 is expressed throughout *Drosophila* oogenesis, but as the oocyte is specified, it shifts from a cytoplasmic to predominantly nuclear localization.³¹ A conserved cofactor called Windei (*wde*) is required for either SETDB1 nuclear translocation or nuclear stability.^{32,33} The loss of *SETDB1* during germline development results in an accumulation of undifferentiated cells.^{29,34} In addition, the loss of *SETDB1* and *wde* also results in egg chambers that do not grow and die during oogenesis.^{28,32} *SETDB1* is known to be required for silencing transposons and male-specific transcripts in the female germ line.^{29,34,35} However, the up-regulation of neither transposons nor male-specific genes in the female germ line results in egg chambers that do not grow.^{36,37} Together, these data suggest that *SETDB1* silences a yet-unidentified group of genes to promote oogenesis.

Here, we find that genes that are expressed in early stages of oogenesis, including genes that promote oocyte differentiation and synaptonemal complex formation, are silenced upon oocyte specification via a feedback loop between *SETDB1*-mediated heterochromatin and the nucleopore complex (NPC). The inability to silence these differentiation-promoting genes due to the loss of either *SETDB1* or members of the NPC results in the loss of oocyte identity and death. Several aspects of germ cell differentiation have been studied and implicated in the loss of fertility in sexually reproducing organisms. Our work indicates that a previously unappreciated broad transcriptional reprogramming silences critical aspects of the germ cell differentiation program at the onset of oocyte specification and is essential to promote oocyte identity.

RESULTS

***SETDB1* promotes the silencing of *RpS19b* reporter at the onset of oocyte specification**

We hypothesized that the expression of early-oogenesis mRNAs, such as *RpS19b*, is silenced upon oocyte specification. To monitor *RpS19b* expression, we used a reporter that expresses an *RpS19b*:GFP fusion protein from the endogenous *RpS19b* promoter. This *RpS19b*:GFP shows high expression in the germarium and attenuated expression post-oocyte specification and in the subsequent egg chambers, consistent with its

endogenous *RpS19b* mRNA expression pattern (Figures 1B–1C1 and 1I).^{22,38}

Using a previously characterized hemagglutinin (HA)-tagged endogenous *SETDB1*, we found that a large fraction of *SETDB1* translocates from the cytoplasm to the nucleus concurrently with oocyte specification (Figures S1A–S1A3).³⁹ To test whether *SETDB1* is required for the silencing of *RpS19b*,^{28,31} we performed germline knockdown (GKD) of *SETDB1* in the background of *RpS19b*:GFP reporter by using two independent RNAi lines. We detected the germ line, *RpS19b*:GFP, and spectrosomes/fusomes/somatic cell membrane in ovaries by immunostaining for Vasa, GFP, and 1B1, respectively.^{40,41} We found that, compared with the control, the GKD of *SETDB1* resulted in ectopic *RpS19b*:GFP protein expression in the differentiated egg chambers without affecting levels in the undifferentiated stages (Figures 1C–1E1, 1H, 1I, and S1B). Thus, *SETDB1* is required for repressing *RpS19b*:GFP reporter in the differentiated egg chambers.

To determine whether nuclear *SETDB1* is required for repressing *RpS19b*:GFP post-oocyte specification, we depleted *wde*, the cofactor required for *SETDB1*'s nuclear localization, in the germ line and independently assayed for *SETDB1* nuclear localization and *RpS19b*:GFP (Figure S1C). The GKD of *wde* resulted in the loss of nuclear *SETDB1* in the differentiated stages of oogenesis without affecting cytoplasmic levels in the undifferentiated stages (Figures S1D–S1F). We found that the GKD of *wde* using two independent RNAi lines, such as the GKD of *SETDB1*, resulted in ectopic *RpS19b*:GFP protein expression in the egg chambers without affecting levels in the undifferentiated stages (Figures 1C–1I). In addition to the upregulation of *RpS19b*:GFP, the GKD of both *SETDB1* and *wde* resulted in egg chambers that did not grow in size and died during oogenesis, as previously reported (Figure S1G).^{28,32} Thus, the repression of the *RpS19b*:GFP reporter in the differentiated egg chambers requires nuclear *SETDB1*.

To further analyze the requirement for *SETDB1* and *wde* in silencing early-oogenesis genes, we generated germline clones of *SETDB1* and *wde* by using the FLP/FRT technique.^{32,42} As the absence of GFP expression marked germline clones, we could not use *RpS19b*:GFP expression as a readout. Instead, we

Figure 1. *SETDB1* and *windei* are required for silencing the *RpS19b* reporter during oogenesis

- (A) A schematic of a *Drosophila* ovariole consisting of germarium and egg chambers surrounded by somatic cells (light red). Egg chambers grow and produce an egg (white).
- (A1) A schematic of a *Drosophila* germarium. Germline stem cells (GSCs; light green) are proximal to somatic niche (red) and divide to give rise to daughter cells called cystoblasts (dark green). Both GSCs and cystoblasts are marked by spectrosomes (red). Cystoblasts differentiate, giving rise to 2-, 4-, 8-, and 16-cell cysts (green), marked by fusomes (red). In the 16-cell cyst, one cell commits to meiosis and specifies an oocyte (dark blue), whereas the other 15 cells become nurse cells (light blue).
- (B–B2) Confocal images of a germarium of a fly carrying *RpS19b*:GFP reporter transgene stained for GFP (green, right grayscale), Egl (red, right grayscale), and Vasa (blue). GFP is expressed in the undifferentiated stages and early cysts (white dashed line), whereas Egl is expressed in the differentiated cysts and localized to the specified oocyte (yellow arrows).
- (C–G1) Ovariole of control *RpS19b*:GFP (C and C1) and GKD of *SETDB1* (D–E1) and *wde* (F–G1) stained for GFP (green, right grayscale), Vasa (blue), and 1B1 (red). Depletion of these genes resulted in egg chambers that ectopically expressed *RpS19b*:GFP (white dashed line), did not grow, and died during oogenesis (white solid arrows).
- (H) Quantification of ovarioles with ectopic *RpS19b*:GFP expression upon the GKD of *SETDB1* or *wde* compared with control ovaries (n = 50 ovarioles; 96% in *SETDB1* GKD #1, 92% in *SETDB1* GKD #2, and 90% in *wde* GKD #1, 70% in *wde* GKD #2 compared with 0% in control). Statistics: Fisher's exact test; **p < 0.001.
- (I) Arbitrary unit (a.u.) quantification of *RpS19b*:GFP expression in the germarium and egg chambers upon the GKD of *SETDB1* (magenta) or *wde* (orange) compared with control ovaries (black). GFP is expressed in the undifferentiated cells and is attenuated in egg chambers. In *SETDB1* and *wde* GKD, GFP expression persists in the egg chambers. Statistics: Dunnett's multiple-comparison test; n = 10 ovarioles; ns, p > 0.05; *p < 0.05; **p < 0.01; ***p < 0.001. Scale bars: 15 μm.

used the expression of another early-oogenesis gene, *blanks*, as a readout.^{16,43} *Blanks* is a component of a nuclear small interfering RNA (siRNA) pathway that has critical roles in the testis but does not have any overt function during oogenesis.⁴³ Although control clones showed no *Blanks* staining in the differentiated egg chamber (Figures S1H and S1H1), mutant clones for *SETDB1* and *wde* showed *Blanks* expression in the differentiated egg chambers (Figures S1I–S1K). Our data suggest that nuclear *SETDB1* is required for silencing early-oogenesis genes, such as *RpS19b* and *blanks*, during oocyte differentiation.

***SETDB1* and *wde* repress genes that are primarily expressed before oocyte specification**

To determine whether *SETDB1* and *wde* repress other differentiation-promoting genes in addition to *RpS19b* and *blanks*, we performed RNA sequencing (RNA-seq). We compared ovaries from *SETDB1*- and *wde*-GKD flies with ovaries from control (*UAS-Dcr2;nosGAL4*) flies, including young virgin flies lacking late-stage egg chambers. Principal-component analysis of the RNA-seq data revealed that *SETDB1*- and *wde*-GKD ovary transcriptomes closely resembled those of young virgin controls rather than those of adult controls (Figure S2A). Using a 1.5-fold cutoff (fold change [FC] $\geq |1.5|$) and false-discovery rate (FDR) < 0.05 , we found that 2,316 genes were upregulated and 1,972 were downregulated in *SETDB1*-GKD ovaries compared with young virgin control ovaries and that 1,075 genes were upregulated and 442 were downregulated in *wde*-GKD ovaries compared with young virgin controls (Figures 2A and 2B; Table S1). Moreover, a comparison of *wde*- and *SETDB1*-GKD ovaries showed a significant overlap of the upregulated (80%) and downregulated (75%) transcripts, suggesting that *SETDB1* and *wde* co-regulate a cohort of genes during oogenesis (Figures 2C and S2B).

SETDB1 and *Wde* are known to repress gene expression; thus, we first focused on mRNAs with increased levels in the GKD ovaries.^{28,33} Gene Ontology (GO) analysis of the shared upregulated RNAs indicated that many were genes involved in differentiation (Figure 2D). Among the upregulated RNAs were *RpS19b* and *blanks*, validating our initial screen, as well as genes that promote synaptonemal complex formation, such as *sunn*, *ord*, and *conA* (Figures 2E, 2F, and S2C–S2E). Thus, *SETDB1* and *wde* repress a cohort of RNAs that are either critical for differentiation or merely expressed during early oogenesis.

To determine when *SETDB1* and *Wde* act to repress genes during oogenesis, we analyzed available RNA-seq libraries enriched for GSCs, cystoblasts, cysts, early egg chambers, and late-stage egg chambers.²² We found that *SETDB1*- and *wde*-regulated RNAs decreased after the cyst stages, and compared with non-target levels, their levels were attenuated in the later stages of oogenesis (Figures 2G, S2F, and S2G).²² This reduction did not happen without *SETDB1* and *wde* (Figure 2G). RNA *in situ* analysis of *blanks* and *RpS19b* revealed that these mRNAs are present in the early stages of oogenesis and are attenuated after oocyte specification in controls, but these RNAs persisted in *SETDB1*- and *wde*-GKD egg chambers (Figures 2H–2O). Thus, mRNAs broadly expressed before oocyte specification are repressed by *SETDB1* and *Wde* in differentiated egg chambers.

***SETDB1* represses the transcription of a subset of targets by increasing H3K9me3 enrichment**

To investigate whether *SETDB1*- and *wde*-regulated mRNAs are repressed at transcriptional level, we examined a subset of nascent transcripts (pre-mRNAs) by qRT-PCR. Indeed, the levels of nascent *RpS19b*, *ord*, *sunn*, *conA*, and *blanks* mRNAs were higher in *SETDB1*- and *wde*-GKD ovaries than in control ovaries (Figures S3A and S3B). These data suggest that transcription of these genes increases upon the loss of *SETDB1* or *wde*. *SETDB1* and its nuclear translocation by *Wde* are required for silencing genes expressed in the early stages of oogenesis. We found that the GKD of *SETDB1* reduced H3K9me3 throughout oogenesis, whereas the GKD of *wde* reduced H3K9me3 in the differentiated egg chambers but not in the undifferentiated stages (Figures S3C–S3F). This suggested that *SETDB1*-mediated H3K9me3 heterochromatin is required for silencing early-oogenesis genes during oocyte differentiation.

To determine whether the *SETDB1*-dependent repression of these genes involves changes in H3K9me3, we performed CUT&RUN^{44,45} on adult control (*UAS-Dcr2;nosGAL4*) ovaries enriched for differentiated egg chambers where these genes are repressed (Figure 2G). Analysis of CUT&RUN data from an adult control showed enrichment of H3K9me3 marks on previously identified *SETDB1* targets and genes containing heterochromatin, such as PHD Finger Protein 7 (*phf7*) and light (*lt*), respectively, validating our CUT&RUN data (Figures 3A, 3B, and S3G).^{34,46} Given that genes in the *Drosophila* genome are closely packed, we analyzed only the gene body from the 5' UTR to the end of the 3' UTR to unambiguously identify *SETDB1*-regulated genes.⁴⁷ We found that, compared with the immunoglobulin G (IgG) negative control, 1,593 out of 2,316 genes upregulated upon the loss of *SETDB1* were enriched for H3K9me3 marks (Figure 3C). In addition, we found that 888 genes lost H3K9me3 on their gene bodies upon the GKD of *SETDB1*, including *RpS19b* and ATP-dependent chromatin assembly factor (Acf) (Figures 3D–3G). The upregulated genes that did not show changes to H3K9me3 marks within the gene body could be regulated by elements outside of the gene body or indirectly. Our data suggest that *SETDB1* is required for H3K9me3 enrichment and the transcriptional repression of a cohort of early-oogenesis genes in the egg chamber.

We next wanted to determine whether the catalytic activity of *SETDB1* is required for its silencing of early-oogenesis genes. The catalytic activity of *SETDB1* family is mediated by a conserved tyrosine (Tyr, Y).^{48,49} By aligning the sequences of the SET domain from different species,^{48–50} as well as using the crystal structure of the SET domain, we identified the catalytic tyrosine of *Drosophila* *SETDB1* that promotes methyltransferase activity to be tyrosine 1050 (Tyr 30, when only the SET domain is considered)⁵⁰ (Figure S3H).

To determine whether the catalytic function of *SETDB1* is required for silencing early-oogenesis genes in the differentiated egg chambers, we created a germline-specific expression (*UASp*) line to generate both a wild-type (WT) *SETDB1* (*UAS-SETDB1^{RNAi-res_WT}-GFP*) and a putative catalytically dead version of *SETDB1* by replacing the predicted catalytic Tyr with an alanine (Y → A) mutation (*UAS-SETDB1^{RNAi-res_Y-A}-GFP*). Both WT *SETDB1* and putative catalytically dead

Developmental Cell

Article

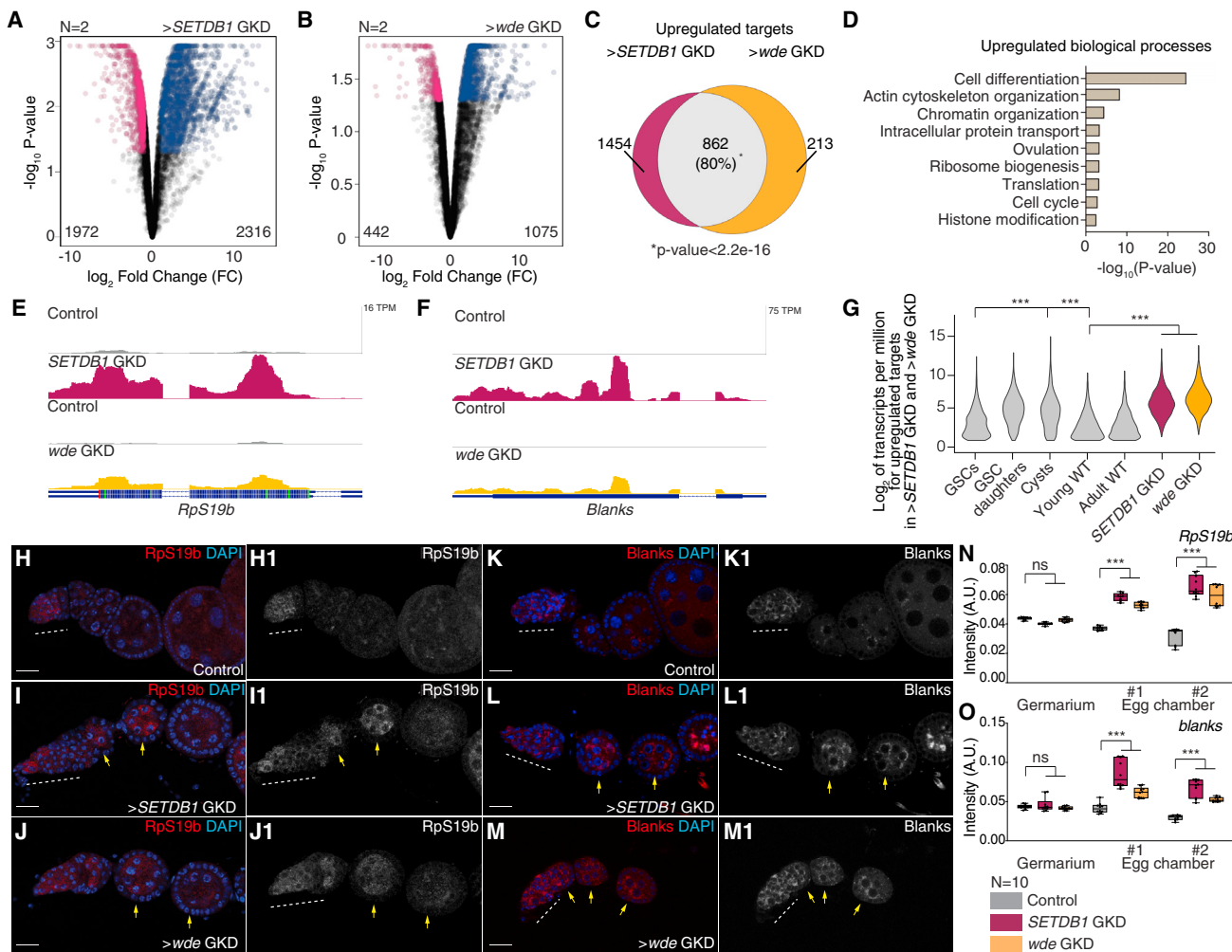


Figure 2. *SETDB1* and *Wde* repress a cohort of early-oogenesis genes

(A and B) Volcano plots of $-\log_{10} p$ value vs. \log_2 fold change (FC) of (A) *SETDB1*-GKD and (B) *wde*-GKD ovaries showing significantly downregulated (pink) and upregulated (blue) transcripts in *SETDB1*- and *wde*-GKD ovaries compared with control ovaries (FDR [false-discovery rate] < 0.05 and genes with 1.5-fold or higher change were considered significant).

(C) Venn diagram of upregulated genes from RNA-seq of *SETDB1*- and *wde*-GKD ovaries compared with controls. 862 targets are shared between the GKD of *SETDB1* and *wde*, suggesting that *SETDB1* and *Wde* co-regulate a cohort of genes.

(D) The biological process GO terms of shared upregulated genes in ovaries depleted of *SETDB1* and *wde* compared with controls (statistics: Fisher's exact test), showing differentiation as one of the significant processes regulated by *SETDB1* and *Wde*.

(G) Violin plot of mRNA levels of the 862 shared upregulated targets in ovaries enriched for GSCs, cystoblasts, cysts, and whole ovaries, showing that the shared

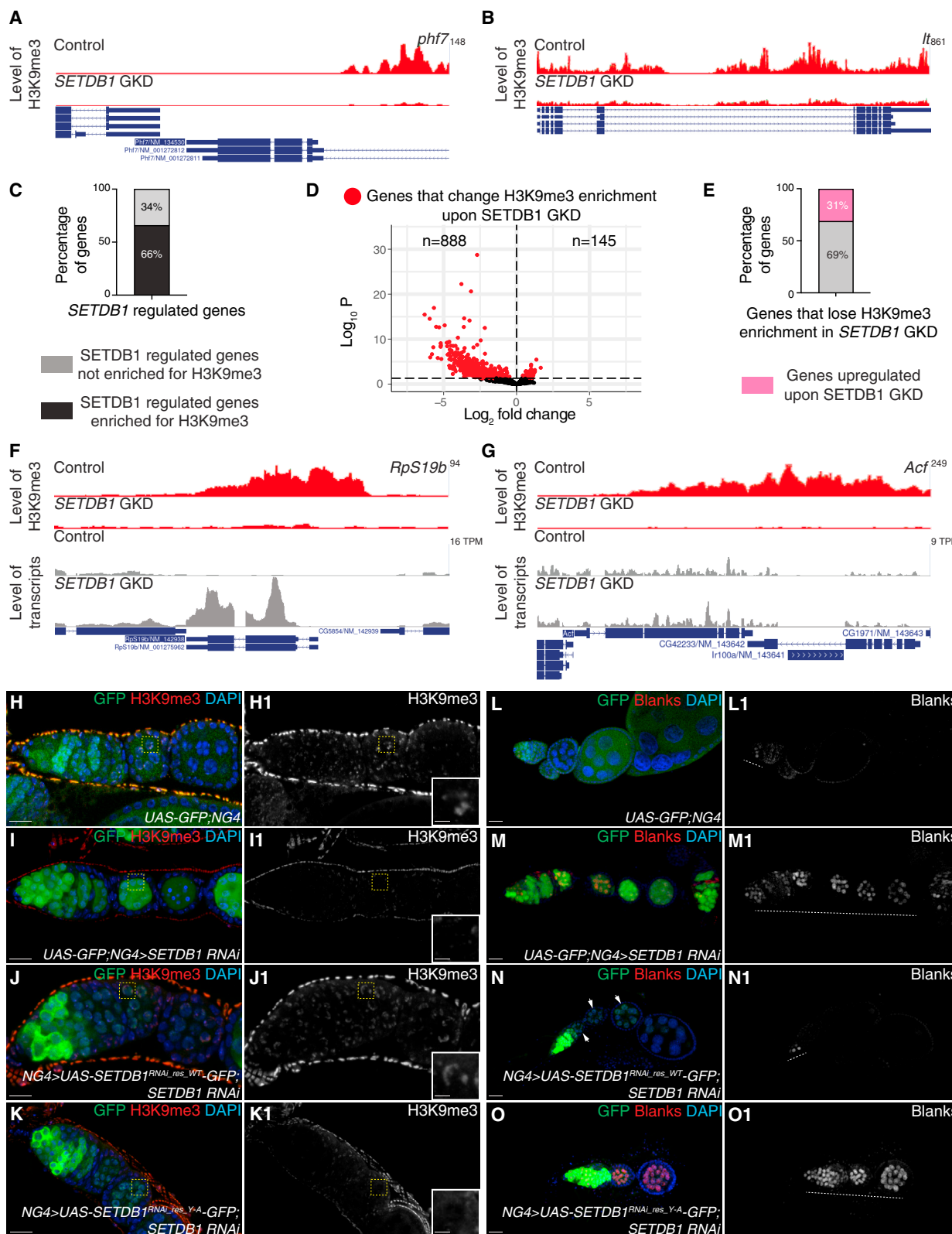
targets between *SETDB1* and *wde* are expressed up to the cyst stages and attenuated in whole ovaries. Statistics: hypergeometric test; ***p < 0.001. (H-J1) Confocal images of germaria probed for *RpS19b* mRNA (red, grayscale) and DAPI (blue) in control (H and H1) showing that *RpS19b* RNA expression

restricted to germanium but in the GKD of *SETDB1* (I and I1) and *wde* (J and J1) ovarioles showing that *RpS19b* mRNA expression is expanded to egg chambers. (K–M1) Confocal images of germania probed for *blanks* mRNA (red, grayscale) and DAPI (blue) in control (K and K1) showing that *blanks* mRNA expression is restricted to early stages of oogenesis and in the GKD of *SETDB1* (L and L1) and *wde* (M and M1) ovarioles, where *blanks* mRNA expression is expanded to egg chambers.

(N and O) Quantification of fluorescence intensity of *RpS19b* (N) and *blanks* (O) mRNAs in the germarium and egg chambers depleted of *SETDB1* (magenta) or *wde* (orange) compared with control ovaries (gray). Statistics: Dunnett's multiple-comparison test; n = 10 ovarioles; ns, p > 0.05; *p < 0.05; **p < 0.01; ***p < 0.001. Scale bars: 15 μ m.

SETDB1 were generated by a transgene that was re-coded via mutations at synonymous sites to make them resistant to RNAi knockdown. We then depleted endogenous *SETDB1* in the germ line by using RNAi and then overexpressed both the WT and putative catalytically dead versions of *SETDB1*.

We stained for H3K9me3 under conditions when only the WT or putative catalytically dead mutant was expressed in the germ line, depleted of endogenous *SETDB1*. We found that the WT *SETDB1* transgene could rescue the endogenous depletion of *SETDB1* and form heterochromatin (Figures 3H–3J1). In



(legend on next page)

Developmental Cell

Article



contrast, the Y→A mutant SETDB1 did not rescue the phenotype and was defective for heterochromatin formation (Figures 3H–3K1). The WT and Y→A mutant SETDB1 were expressed in the germ line and translocated to the nucleus during differentiation (Figures 3J–3K1). Assaying for Blanks expression, we found that WT SETDB1, but not the Y→A mutant SETDB1 transgene, silenced Blanks expression in the differentiated egg chambers (Figures 3L–3O1). Our data suggest that Tyr 1050 contributes to the catalytic activity of SETDB1 and is necessary for silencing early-oogenesis genes, such as *blanks*.

SETDB1 is required for transposon repression during oogenesis,^{29,51} and the upregulation of transposons can affect gene expression.^{52,53} However, we found that the upregulation of genes in the differentiated stages that we observed upon the depletion of *SETDB1* was not due to the secondary effect of transposon upregulation given that the expression of *RpS19b* reporter was not altered in the germ line depleted of *aubergine* (*aub*), a critical component of the piRNA pathway (Figures S3I–S3K),^{35,36,54} nor did *aub* depletion cause mid-oogenesis death as we observed in *SETDB1* and *wde* GKD (Figures S3I–S3K).^{54,55} Overall, our data suggest that the loss of *SETDB1* de-represses a subset of genes during late oogenesis independent of transposon dysregulation.

***SETDB1* is required for the expression of NPC components**

GO term analysis of downregulated targets of *SETDB1* and *wde* GKD included genes that regulate transposition, consistent with the previously described role of *SETDB1* and *Wde* in the piRNA pathway and those that regulate proper oocyte development, consistent with the previously described phenotype (Figure 4A).^{29,31,32,51}

Unexpectedly, we observed that genes involved in nucleocytoplasmic transport were downregulated in *SETDB1*- and *wde*-GKD ovaries compared with control ovaries (Figure 4A). Nucleocytoplasmic transport is mediated by NPCs, which span the nuclear membrane and consist of a cytoplasmic ring, a central scaffold spanning the nuclear envelope, and a nuclear ring and basket (Figure 4B).^{56–58} Beyond regulating nucleocytoplasmic transport, NPCs also regulate gene transcription by anchoring and maintaining heterochromatic domains.^{59–61} We found that the GKD of *SETDB1* and *wde* in the germ line resulted

in the downregulation of 18 out of ~30 nucleoporins (*Nups*) that make up the NPC (Figure 4C), including a germline-enriched *Nup154*, which is critical for oogenesis.^{62–64} The *Nups* that were downregulated upon the depletion of *SETDB1* and *wde* were not isolated to one specific NPC subcomplex (Figures 4B and 4C).

We found that nascent mRNAs corresponding to the *SETDB1* and *wde* targets *Nup154*, *Nup205*, and *Nup107* were downregulated in *SETDB1*- and *wde*-GKD ovaries, whereas the non-target *Nup62* was unaffected, suggesting that *SETDB1* and *Wde* promote the transcription of a cohort of *Nups* (Figure 4D). In addition, the levels of a *Nup107*:RFP fusion protein, under endogenous control,⁶⁵ were significantly lower in the cysts and egg chambers of *SETDB1*- and *wde*-GKD ovaries than in the controls (Figures S4A–S4D).

To determine whether the loss of *Nup* expression in *SETDB1*- and *wde*-GKD ovaries resulted in the loss of NPC formation, we performed immunofluorescence with an antibody that is known to mark NPCs in *Drosophila*.^{56,66} We found that germline NPC levels were lower in the egg chambers of *SETDB1*- and *wde*-GKD ovaries than in the controls (Figures 4E–4H), but the NPCs in the soma were unaffected (Figures 4I and S4E–S4G2), and nuclear laminae were also unaffected (Figures S4H–S4K). Thus, *SETDB1* and *wde* are required for the expression of a subset of *Nups* and NPC formation after oocyte specification.

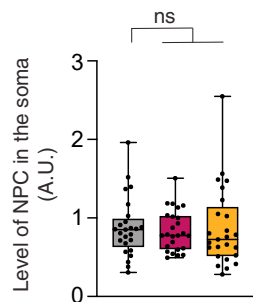
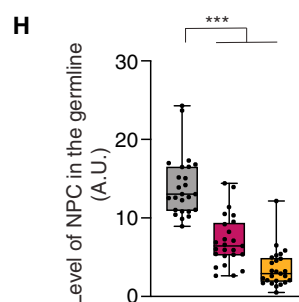
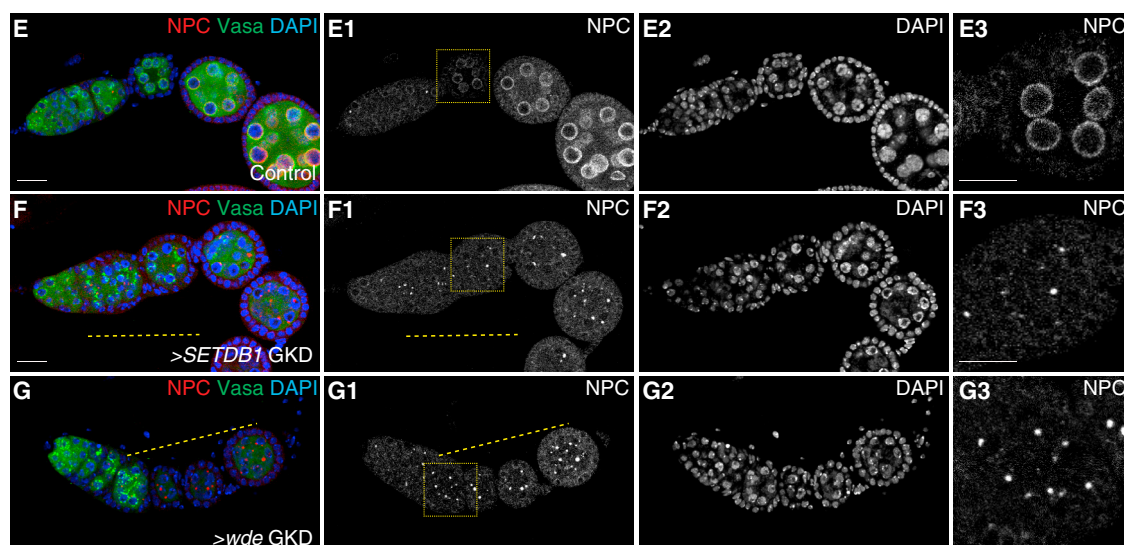
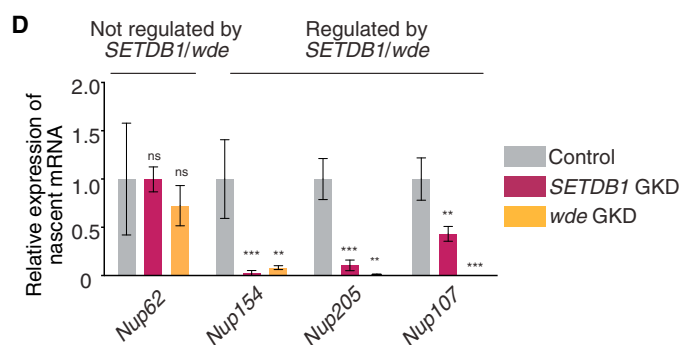
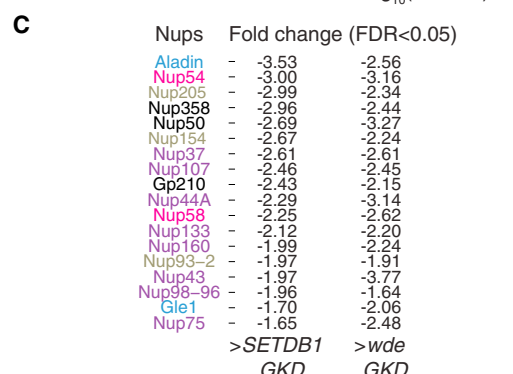
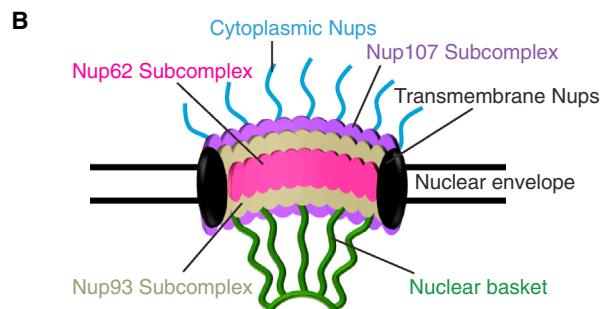
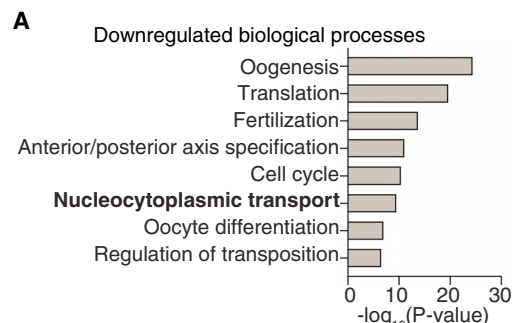
Heterochromatic genes and piRNA clusters require heterochromatin to promote their transcription.^{29,67} Although we found that *SETDB1* is required for the upregulation of *Nups*, CUT&RUN analysis of H3K9me3 marks revealed that only three of the *Nup* genes had any enrichment of H3K9me3 (*Mbo*, *Nup188*, and *Gp210*). Moreover, among *SETDB1*-regulated *Nups*, only *Gp210* showed any heterochromatic enrichment (Table S2). Altogether, we find that *SETDB1* indirectly promotes proper *Nup* expression by a yet unknown mechanism in the germ line.

Nucleoporins are required for maintaining heterochromatin domains at the nuclear periphery

Our data indicate that, in the *Drosophila* female germ line, heterochromatin formation mediated by *SETDB1* is required for proper NPC formation by promoting proper expression of a subset of *Nups*, including *Nup107* and *Nup154* (Figure 4C). In yeast, a subset of *Nups* is part of the heterochromatin proteome and is

Figure 3. *SETDB1* promotes the silencing of early-oogenesis genes by regulating the levels of H3K9me3

(A and B) Tracks showing the level of H3K9me3 on previously validated and known heterochromatic genes *phf7* and *It*, respectively. (C) Bar graph showing genes regulated by *SETDB1* that are enriched for H3K9me3 on the gene body. 1,593 (black) out of 2,316 (gray) genes upregulated upon the loss of *SETDB1* are enriched for H3K9me3. (D) Volcano plot showing changes in H3K9me3 in *SETDB1* GKD compared with WT. 888 genes lose H3K9me3 after *SETDB1* GKD (red). (E) Bar graph showing that 270 (pink) out of 886 (gray) genes that lose H3K9me3 enrichment in *SETDB1* GKD were upregulated upon the loss of *SETDB1*. (F and G) Tracks showing the level of H3K9me3 on target genes (top panel, red) and level of their transcripts in *SETDB1* GKD (bottom panel, gray). The loss of H3K9me3 on *SETDB1* targets *RpS19b* (F) and *Acf* (G), suggesting that they are directly regulated by *SETDB1*. (H–K1) Ovariole from control (H and H1) and the GKD of *SETDB1* (I and I1) in the background of the *UAS-GFP* transgene. RNAi-resistant WT *SETDB1::GFP* transgene (J and J1) and RNAi-resistant Y→A point-mutant *SETDB1::GFP* transgene (K and K1) were stained for GFP (green), H3K9me3 (red), and DAPI (blue). Depletion of *SETDB1* results in the loss of H3K9me3 expression, which was rescued by the WT-*SETDB1* transgene but not the Y→A point mutant (100% in control, 97% in WT *SETDB1::GFP*, and 0% in Y→A point-mutant *SETDB1* transgene; n = 30). (L–O1) Ovariole from control (L and L1) and the GKD of *SETDB1* (M and M1) in the background of *UAS-GFP*. RNAi-resistant WT-*SETDB1* transgene (N and N1) and RNAi-resistant Y→A point-mutant *SETDB1* transgene in the background of *SETDB1* GKD (O and O1) were stained for GFP (green), Blanks (red), and DAPI (blue). Depletion of germline *SETDB1* results in ectopic Blanks expression, which was rescued by the WT but not in the Y→A point-mutant transgene (100% in control, 93% in WT *SETDB1::GFP*, and 3% in Y→A point-mutant *SETDB1* transgene, n = 30). Scale bars: 15 μm.



N=7

- Control
- SETDB1 GKD
- wde GKD

required for clustering and maintaining heterochromatin at the NPC.^{61,68,69} This subset includes Nup107 and the yeast homolog of Nup154, Nup155, both of which have lower expression in *SETDB1*- and *wde*-GKD ovaries than in controls. We hypothesized that in *Drosophila*, *SETDB1* could promote the silencing of early-oogenesis genes by promoting heterochromatin formation. This heterochromatin then promotes the expression of Nups and NPC formation, which can help maintain heterochromatin by anchoring it to nuclear periphery, thus promoting the silencing of early-oogenesis genes.

To first determine whether heterochromatin and Nups associate in the *Drosophila* female germ line, we utilized antibody against H3K9me3 to mark heterochromatin and Nup107::RFP to mark NPCs in control ovarioles (*nosGAL4*; *Nup107-RFP*).^{29,65} We found that H3K9me3 domains were often at the nuclear periphery, proximal to Nup107::RFP (Figures 5A–5A2 and 5C). Next, to determine whether the loss of Nups leads to the loss of heterochromatin, we first depleted *Nup154* and probed for heterochromatin formation. We chose *Nup154* because its loss-of-function phenotype has been well described.^{63,64} We found that the GKD of *Nup154* in the germ line resulted in egg chambers that did not grow and died during oogenesis, as previously described for *Nup154* mutants (Figures S5A–S5C).⁶³ In addition, upon the depletion of *Nup154*, the translocation of *SETDB1* from the cytoplasm to the nucleus, monitored by immunostaining, was not affected, suggesting that the attenuation of heterochromatin upon the GKD of Nups is not due to the loss of transport of *SETDB1* into the nucleus (Figures S5D–S5F). By staining for H3K9me3 marks, we found that upon the GKD of *Nup154*, heterochromatin domains initially formed (Figures S5G–S5H3). However, in the egg chambers of *Nup154* GKD, the colocalization between H3K9me3 domains and Nup107::RFP levels at the nuclear periphery were significantly reduced before the reduction of heterochromatin levels (Figures 5A–5C and S5G–S5H3). The GKD of *Nup107* also resulted in egg chambers that did not grow and lost heterochromatin (Figures S5F–S5K). Moreover, the loss of germline *Nup154* resulted in an increased distance between heterochromatin domains and the nuclear periphery marked by lamin C (Figures 5D–5F). Thus, *Nup154* and *Nup107*, positively regulated by *SETDB1*, are required for H3K9me3 localization at the nuclear periphery for H3K9me3 maintenance in the female germ line.

Nups are required for silencing early-oogenesis genes

On the basis of our above findings that Nups are required for maintaining H3K9me3 levels and localization, we hypothesized that they are also required for silencing the early-oogenesis RNAs in differentiated egg chambers. To test this hypothesis, we depleted *Nup154* and *Nup107* in the germ line of a fly carrying the *RpS19b::GFP* reporter. We found that the GKD of these Nups resulted in the upregulation of *RpS19b::GFP*, phenocopying the GKD of *SETDB1* and *wde* (Figures 6A–6C, S6A–S6B1, and S6D). Moreover, the germline depletion of *Nup62*, which is within the NPC but not regulated by *SETDB1*, also resulted in the upregulation of *RpS19b::GFP* and egg chambers that did not grow (Figures S6A–S6D). This suggests that the activity of NPC components, and not just the Nups regulated by *SETDB1*, is required for silencing the *RpS19b::GFP* reporter.

To determine whether Nups are required for silencing other early-oogenesis RNAs, we performed RNA-seq and compared *Nup154*-GKD ovaries with young ovaries (*UAS-Dcr2;nosGAL4*) as a developmental control (Figure S2A). Using a 1.5-fold cutoff ($FC \geq |1.5|$ and $FDR < 0.05$), we found that compared with the control, *Nup154*-GKD ovaries showed 2,809 upregulated genes and 2,922 downregulated genes (Figure 6D) (Table S1). Strikingly, 97% of the upregulated genes and 89% of the downregulated *SETDB1* and *wde* targets overlapped with *Nup154* GKD (Figures 6E and S6E). *Nup154* was involved in silencing genes that promote oocyte differentiation, including synaptonemal complex components *ord*, *sunn*, *conA*, and *RpS19b* (Figures 6F and S6F–S6H). In addition, the GKD of *Nup154* also resulted in the upregulation of *blanks* (Figure S6I). The levels of *Nup154*-regulated RNAs decreased after the cyst stage, when the oocyte is specified, whereas non-targets had similar RNA levels at all stages (Figures 6G, S6J, and S6K). Thus, *Nup154* is critical for silencing early-oogenic mRNAs in the differentiated egg chambers.

To determine whether *Nup154* is required for H3K9me3 marks at *SETDB1*-regulated gene loci, such as *RpS19b*, we carried out CUT&RUN for H3K9me3 in control and *Nup154*-GKD ovaries. We found that 564 out of 622 genes displaying a loss in H3K9me3 in *Nup154* GKD also showed the same loss in *SETDB1* GKD, including *RpS19b* and *Acf* (Figures 6H, S6L, and S6M; Table S2). We conclude that Nups are required for silencing and maintaining H3K9me3 at a subset of *SETDB1*- and *wde*-regulated loci.

Figure 4. *SETDB1* and *Wde* promote the expression of a subset of nucleoporin genes and NPC formation

- (A) The significant biological process GO terms of downregulated genes in *SETDB1*- and *wde*-GKD ovaries compared with controls (FDR from p values using a Fisher's exact test), showing nucleocytoplastic transport as one of the processes regulated by *SETDB1* and *Wde*.
- (B) A schematic of the nucleoporin complex (NPC) composed of ~30 nucleoporins (Nups) and organized into subcomplexes.
- (C) Table showing the levels of 18 nucleoporin mRNAs that are downregulated 1.5-fold or more in both *SETDB1*- or *wde*-GKD ovaries compared with control ovaries.
- (D) qRT-PCR assay showing that the pre-mRNA levels of *SETDB1*- and *Wde*-regulated *Nup* genes, including *Nup154*, *Nup205*, and *Nup107*, are lower than those of controls, whereas the levels of non-target *Nup62* pre-mRNA are not affected (control level vs. *SETDB1*-GKD and *wde* RNA, n = 3, **p < 0.01; ***p < 0.001; error bars are SEM, Student's t test).
- (E–G) Ovariole and egg chamber images of controls (E–E3) and the GKD of *SETDB1* (F–F3) and *wde* (G–G3) stained for NPC (red, grayscale), Vasa (green), and DAPI (blue). NPC staining was done with Mab414 antibody. Depletion of *SETDB1* and *wde* shows reduced expression of NPC in the egg chambers, suggesting that *SETDB1* regulates the expression of several nucleoporins, which in turn regulates the formation of NPC.
- (H–I) Arbitrary unit (a.u.) quantification of NPC level in the germ line (H) and soma (I) in *SETDB1*- and *wde*-GKD ovaries compared with controls. Statistics: Dunnett's multiple-comparison test; n = 25 ovariole for germ line and 15 for somatic quantitation; ns, p > 0.05; *p ≤ 0.05; **p < 0.01; ***p < 0.001. Scale bars: 15 μm in main images and 4 μm in insets.

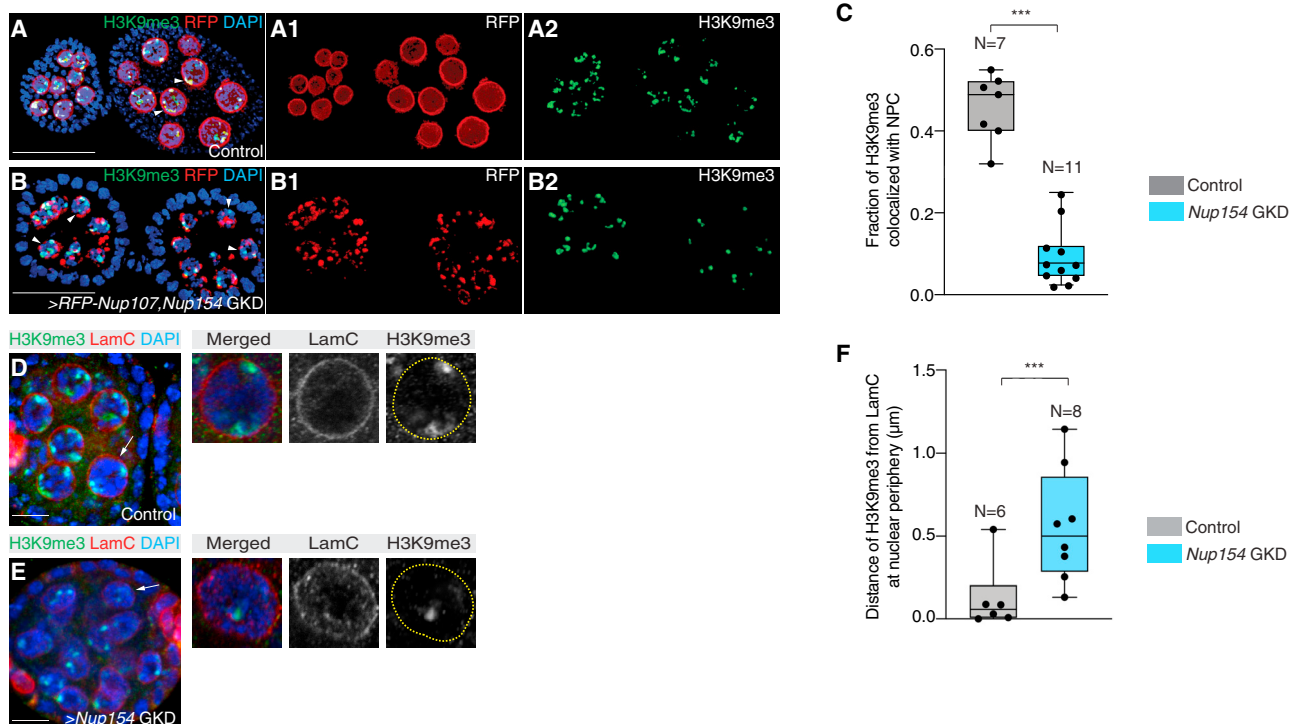


Figure 5. H3K9me3 heterochromatin colocalizes with NPC component Nup107 at the nuclear periphery

(A–A2) Egg chambers of control ovariole showing RFP-Nup107 (red, right red channel) and H3K9me3 (green, right green channel). Heterochromatin is seen in close association with NPC (white arrows). Colocalized fraction is shown in yellow.

(B–B2) Egg chambers of *Nup154* GKD ovariole showing significant decrease in the colocalization (white arrows) between RFP-Nup107 (red, right red channel) and H3K9me3 (green, right green channel).

(C) Quantification of the fraction of H3K9me3 that colocalizes with NPC in the germ line of control ovarioles (gray) in contrast to *Nup154* GKD ovarioles (blue). Quantitative object-based colocalization was measured in Imaris software; *** $p < 0.001$, one-tailed Student's t test.

(D and E) Egg chambers of control (**D**) and *Nup154* GKD (**E**) ovarioles showing significant increase in the distance between LamC (red) and H3K9me3 (green). Single nuclei from control and *Nup154* GKD ovarioles are shown in the insets.

(F) Quantification of distance between H3K9me3 and LamC in the germ line of control ovarioles (gray) in contrast to *Nup154* GKD ovarioles (blue). Statistics: *** $p < 0.001$, one-tailed Welch's t test.

Scale bars: 15 μ m.

To ascertain whether the loss of proper NPC formation results in the mis-localization of heterochromatin targets, such as *RpS19b*, from the nuclear periphery, we performed DNA *in situ* hybridization of the gene locus by using *RpS19b* DNA probes.^{70–72} *In situ* hybridization and staining for nuclear lamina with lamin C antibody showed the presence of this gene locus proximal to nuclear lamina in the control (Figures 6I–6L2). However, the loss of *Nup154* in the germ line resulted in an increased distance between the *RpS19b* locus and nuclear lamina (Figures 6I–6K). This suggests that after oocyte specification, proper formation of NPC is required for maintaining *RpS19b* locus at the nuclear periphery.

NPC loss affects H3K9me3 heterochromatin but not H3K27me3 heterochromatin

H3K27me3 can also promote silencing during *Drosophila* oogenesis.^{73,74} NPC is required for maintaining SETDB1-deposited H3K9me3 heterochromatin by anchoring it to the nuclear periphery. To determine whether NPC also promotes H3K27me3 gene-silencing marks, we stained for H3K27me3

in both *SETDB1* and *Nup154* GKD. We found that the H3K27me3 level increased upon the germline loss of *SETDB1* and *Nup154* (Figures S7A–S7D). This suggests that the effects of *SETDB1* and *Nup154* are specific to H3K9me3 but not H3K27me3 repressive marks.

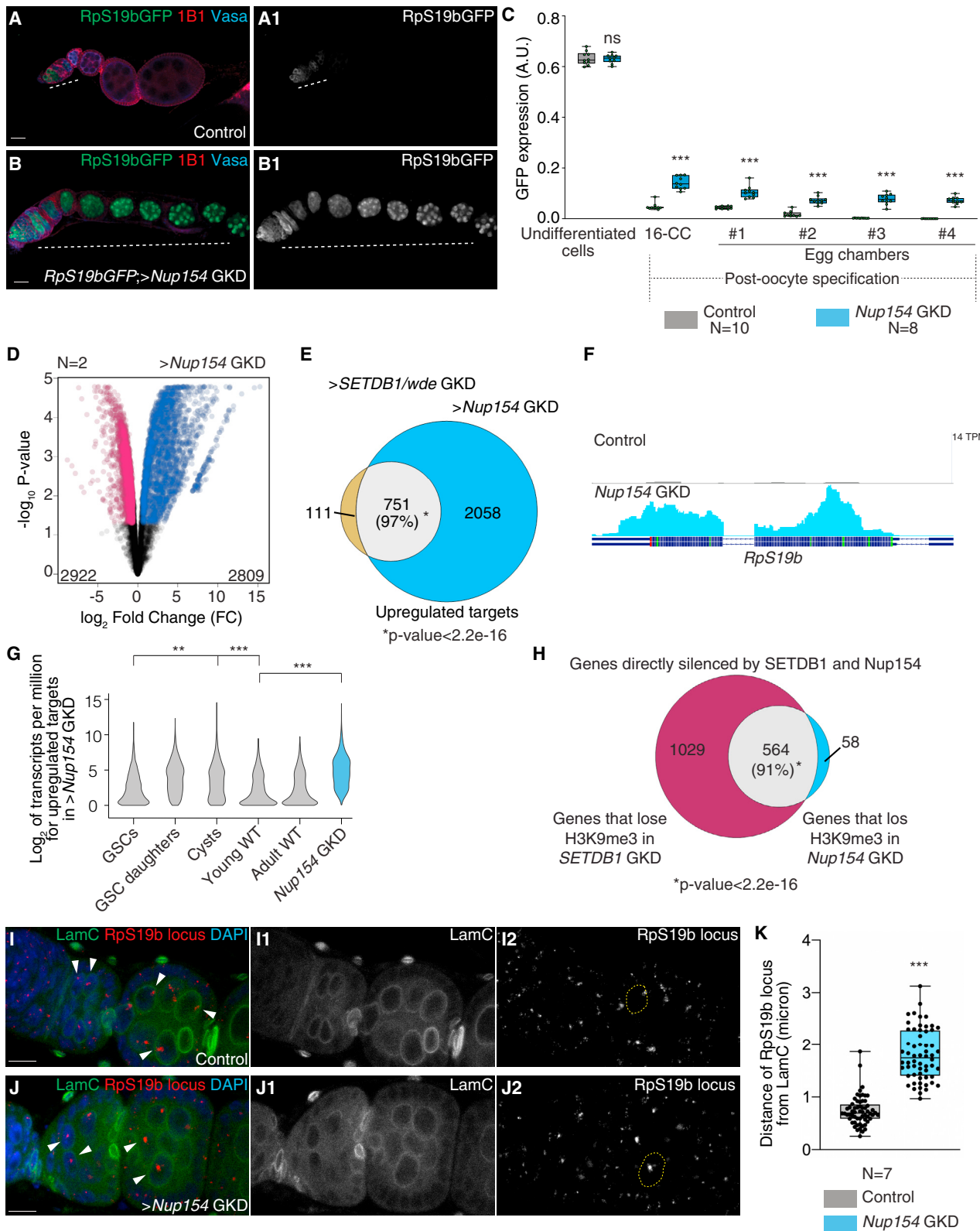
Silencing genes expressed during the early-oogenesis stages is required for maintaining oocyte fate

We next asked why the loss of *SETDB1*, *wde*, and *Nups* results in egg chambers that do not grow and die during oogenesis. Egg chambers with oocyte specification or maintenance defects die during oogenesis.¹⁶ To determine whether there are oocyte specification or maintenance defects, we stained the GKD of *SETDB1*, *wde*, and *Nup154* for the oocyte marker Egl, as well as Vasa and 1B1.^{14,15} In the early stages of oogenesis, as in the control, the GKD of *SETDB1*, *wde*, and *Nup154* caused Egl to seemingly localize to one cell (Figures 7A–7E). However, in the later egg chambers, compared with the control ovariole, the GKD of *SETDB1*, *wde*, and *Nup154* resulted in either mis-localization or diffused Egl expression, suggesting the loss of

Developmental Cell

Article

CellPress



(legend on next page)

oocyte fate (Figures 7A–7E). Thus, *SETDB1*, *wde*, and *Nup154* are required for maintaining an oocyte fate.

DISCUSSION

Many maternally contributed mRNAs in oocytes are critical for early development after fertilization.^{13,14,75–77} We previously showed that many mRNAs expressed in germ cells and the undifferentiated stages of oogenesis must be selectively degraded and thus excluded from the maternal contribution.¹⁶ However, the potential role of the transcriptional silencing of germ cell and GSC-enriched genes during oogenesis was unclear. Here, we have found that regulated translocation of *SETDB1* into the nucleus during oocyte specification is required for silencing germ cell and early-oogenesis genes in the differentiated egg chambers (Figure 7F) and that this process is essential to maintaining oocyte fate. Thus, some genes expressed in germ cells and some that promote differentiation are transcriptionally silenced at the onset of oocyte specification mediated by a feedback loop between heterochromatin and NPC.

Regulated heterochromatin formation during oocyte specification promotes the germ-cell-to-oocyte transition

A large fraction of *SETDB1* is cytoplasmic in the undifferentiated stages of the germ line. As the oocyte is specified during differentiation, *SETDB1* becomes mostly nuclear.²⁸ This translocation of *SETDB1* to the nucleus during oocyte specification is mediated by *Wde*, the *Drosophila* ortholog of mAM/MCAF1.^{32,33} Here, we find that the translocation of *SETDB1* to the nucleus during oocyte specification is required for silencing germ cell and early-oogenesis genes at the onset of oocyte specification. MCAF1 also regulates the accumulation of *SETDB1* in the nucleus in mammalian cells.⁷⁸ In addition, the loss of *SETDB1* during mammalian oogenesis results in meiotic defects and infertility.⁷⁹ These data suggest that regulated heterochromatin formation to promote the silencing of early-oogenesis genes could be conserved to regulate oogenesis in mammals.

We discovered that *SETDB1* is required for silencing two major classes of genes. The first group is involved in GSC differentiation into an oocyte, including critical genes that promote meiosis I. The second group of genes are those that are expressed in the germ cells before differentiation into an oocyte but have no specific function in the female germ line, such as *blanks*.^{16,43} We propose that these genes silenced upon oocyte specification are detrimental to late oogenesis or early embryogenesis. Indeed, it has been shown that overexpression of one such gene, *actin 57B* (*act57B*), which is repressed by *SETDB1* and *Wde* (Table S1), is detrimental to oogenesis.^{16,80} Remarkably, some of the mRNAs encoded by genes that *SETDB1* transcriptionally silences during this transition are also targeted at the post-transcriptional level for degradation by members of the no-go decay pathway, such as *blanks* and *Act57B*.¹⁶ Thus, our data suggest that the regulation of gene expression during oocyte differentiation reflects a two-step process: transcriptional silencing dependent on *SETDB1* and post-transcriptional degradation of mRNAs to exclude a cohort of germ cell mRNAs from the maternal contribution.¹⁶

Nucleopore complex and heterochromatin are in a feedback loop to promote gene silencing

The NPC not only mediates selective nucleo-cytoplasmic transport of macromolecules but also regulates gene expression by anchoring chromatin domains, including heterochromatin, to the nuclear periphery.^{61,81,82} In addition, several Nups are also part of the heterochromatin proteome in yeast, suggesting that NPCs can regulate gene expression by regulating heterochromatin.^{61,83} Consistent with these observations, we find that NPC and heterochromatin are closely associated in the female germ line of *Drosophila*. The loss of NPCs due to the depletion of individual Nups results in the loss of heterochromatin and subsequent upregulation of germ cell and early-oogenesis genes, resulting in oogenesis defects. The large overlap of target genes among *SETDB1*, *wde*, and *Nup154* indicates that Nups are functioning in the same pathway as *SETDB1*. This suggests that not only do NPCs associate with heterochromatin, but they also play

Figure 6. *Nup154* is required for silencing a cohort of genes expressed during early oogenesis

(A–B1) Ovariole of control *RpS19b::GFP* (A and A1) and GKD of *Nup154* (B and B1) stained for GFP (green, right grayscale), Vasa (blue), and 1B1 (red). Depletion of *Nup154* results in the ectopic expression of *RpS19b::GFP* (white dashed line) and egg chambers that did not grow.

(C) a.u. quantification of *RpS19b::GFP* expression in the germarium and egg chambers upon the GKD of *Nup154* (blue) compared with a control (gray). GFP is expressed in the germarium and then attenuated upon egg chamber formation in the control. In *Nup154* GKD, GFP expression persists in the egg chambers. Statistics: Dunnett's multiple-comparison test; n = 10 and 8 ovarioles for control and *Nup154* GKD, respectively; ns, p > 0.05; *p < 0.05; **p < 0.01, ***p < 0.001.

(D) Volcano plots of $-\log_{10}p$ value vs. \log_2FC of mRNAs that show significantly downregulated (pink) and upregulated (blue) transcripts in *Nup154* GKD ovaries compared with control ovaries (FDR < 0.05 and 1.5-fold or higher change were considered significant).

(E) Venn diagram of upregulated overlapping genes from the RNA-seq of *SETDB*-GKD, *wde*-GKD, and *Nup154*-GKD ovaries compared with controls. 751 upregulated targets are shared among *SETDB1* GKD, *wde* GKD, and *Nup154* GKD, suggesting that *Nup154* and *SETDB1* function to co-regulate a cohort of genes.

(F) RNA-seq track showing that *RpS19b* is upregulated upon the germline depletion of *Nup154*.

(G) Violin plot of mRNA levels of the 2,809 upregulated targets in ovaries enriched for GSCs, cystoblasts, cysts, and whole ovaries, showing that the upregulated targets of *Nup154* are most highly enriched up to the cyst stages and then attenuated in whole ovaries. Statistics: hypergeometric test; ***p < 0.001.

(H) Venn diagram showing overlapping genes that lose H3K9me3 after the depletion of both *SETDB1* and *Nup154* in the germ line. 622 genes lose H3K9me3 after *Nup154* GKD, out of which 564 genes are also directly silenced by *SETDB1*, suggesting co-regulation of these genes by both *SETDB1* and *Nup154*.

(I–J2) Ovariole of control (I–J2) and the GKD of *Nup154* (J–J2) probed for *RpS19b* genomic locus (red, right grayscale) by DNA *in situ* and stained for LamC (green, right grayscale) and DAPI (blue). Depletion of *Nup154* shows increased distance of *RpS19b* locus from nuclear periphery in nurse cells (white arrows). One nurse cell nucleus is shown with a yellow dotted circle for both control and *Nup154* GKD.

(K) Quantitation of the distance between *RpS19b* locus from the nuclear periphery in nurse cells of control (gray) and *Nup154* GKD (blue) in microns. Distance was measured in ImageJ using the straight-line function. Statistics: ns, p > 0.05; *p < 0.05; **p < 0.01; ***p < 0.001, Welch's t test.

Scale bars: 15 μ m.

Developmental Cell

Article

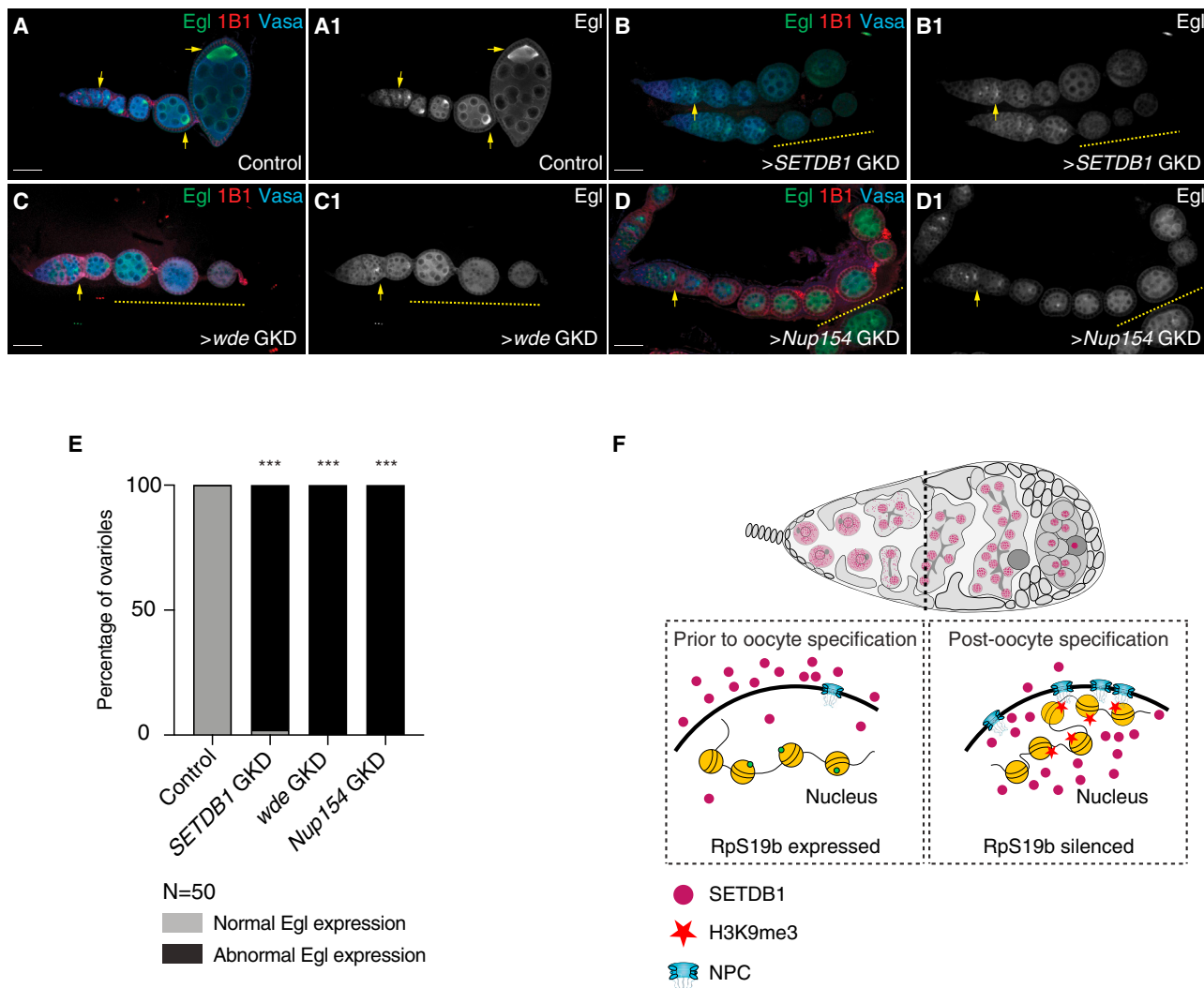


Figure 7. Silencing of early-oogenesis genes mediated by SETDB1, Wde, and Nup154 is required for the maintenance of oocyte fate

(A–D1) Ovarioles of a control (A and A1) and the GKD of *SETDB1* (B and B1), *wde* (C and C1), and *Nup154* (D–D1) stained for Egl (green, right grayscale), Vasa (blue), and 1B1 (red). The control shows proper oocyte specification, whereas the depletion of *SETDB1*, *wde*, and *Nup154* in the germ line results in initial oocyte specification (yellow arrow), which is then lost in the subsequent egg chambers (yellow dashed line).

(E) Quantification of the percentage of ovarioles with abnormal or loss of Egl expression (black) in ovaries depleted of *SETDB1*, *wde*, or *Nup154* compared with control ovaries (gray) ($n = 50$ ovarioles; 98% in *SETDB1* GKD and 100% in *wde* GKD and *Nup154* GKD compared with 0% in the control). Statistics: Fisher's exact test. *** $p < 0.001$.

(F) A model showing that nuclear *SETDB1* after differentiation promotes heterochromatin formation. This heterochromatin promotes NPC formation, which in turn helps maintain heterochromatin.

Scale bars: 15 μ m.

a role in maintaining heterochromatin and gene repression during oocyte differentiation.

The number of genes that need to be silenced varies by cell type and developmental trajectory. How the levels of heterochromatin are coupled to their NPC docking sites in the cell was not known. Like heterochromatin levels, the number of NPCs varies by cell type and during differentiation.⁸⁴ How the NPC number is regulated during development was not fully understood. Our findings in the female germ line suggest an elegant tuning mechanism for heterochromatin and its NPC docking sites. Heterochromatin promotes the levels of NPC, which then

promote heterochromatin maintenance by tethering it to the nuclear periphery. We find that this loop can be developmentally regulated by Wde-mediated control of the levels of *SETDB1* in the nucleus to promote heterochromatin formation.

Limitations of the study

We do not know how *SETDB1* is guided to its targets to promote their silencing. Similarly, what triggers *SETDB1* translocation from the cytoplasm to the nucleus during oocyte specification and thus promotes the heterochromatinization of early-oogenesis genes is not known. The loss of *SETDB1* results in the

upregulation of a large set of early-oogenesis genes, but we find that a cohort of these upregulated genes are the direct targets with heterochromatin on their gene body, such as *Rps19b*. We do not know how SETDB1 controls the silencing of targets such as *banks*. Lastly, we find that SETDB1 promotes the expression of Nups and that Nup genes are not heterochromatic genes. We speculate that SETDB1 regulates NPC formation indirectly, but the mechanism is not known. Finally, it is possible that multiple Nups but not all Nups are required in silencing early-oogenesis genes during oocyte differentiation.

STAR★METHODS

Detailed methods are provided in the online version of this paper and include the following:

- KEY RESOURCES TABLE
- RESOURCE AVAILABILITY
 - Lead contact
 - Materials availability
 - Data and code availability
- EXPERIMENTAL MODEL AND STUDY PARTICIPANT DETAILS
 - Husbandry conditions of experimental animals
 - Fly lines
- METHOD DETAILS
 - UAS-SETDB1-GFP overexpression line construction
 - Dissection and Immunostaining
 - Fluorescence imaging
 - Egg laying assays
 - RNA isolation
 - RNA-seq library preparation and analysis
 - Fluorescent *in situ* hybridization
 - CUT&RUN assay
 - DNA seq library preparation and analysis
 - CUT&RUN data analysis
 - Quantitative Real Time-PCR (qRT-PCR)
- QUANTIFICATION AND STATISTICAL ANALYSIS
 - Quantifications of egg chamber area and fluorescent intensity
 - Colocalization analysis
 - Quantification of H3K9me3 mark distance from nuclear periphery

SUPPLEMENTAL INFORMATION

Supplemental information can be found online at <https://doi.org/10.1016/j.devcel.2023.08.014>.

ACKNOWLEDGMENTS

We are grateful to all members of the Rangan laboratory and Drs. Thomas Hurd, Miller Lee and Flo Marlow for discussion and comments on the manuscript. We also thank the Sontheimer lab, Lehmann lab, and Wodarz lab for flies and antibodies; the Joyce lab for probes; and the Bloomington Drosophila Stock Center, the Vienna Drosophila Resource Center, the Transgenic GKD Project (NIH/NIGMS R01-GM084947), the BDGP Gene Disruption Project, and FlyBase for fly stocks and reagents. P.R. is funded by NIH/NIGMS (R01GM11177 and R01GM135628), M.A.S. is funded by NIH NIGMS R35 138120, and A.M.V. is funded by R01DE030927.

AUTHOR CONTRIBUTIONS

Conceptualization, P.R. and K.S.; methodology, P.R. and K.S.; software, A.L. and M.A.S.; formal analysis, K.S., A.L., E.T.M., and M.A.S.; investigation, K.S., N.M.K., A.L., J.C., A.I., and A.M.; resources, K.S. and P.R.; data curation, K.S., A.M.V., and M.A.S.; writing – original draft, P.R. and K.S.; writing – review & editing, P.R., A.M.V., M.A.S., and K.S.; visualization, K.S. and A.M.V.; supervision, P.R.; project administration, P.R.; funding acquisition, P.R.

DECLARATION OF INTERESTS

The authors declare no competing interests.

Received: November 2, 2021

Revised: April 12, 2023

Accepted: August 9, 2023

Published: September 5, 2023

REFERENCES

1. Seydoux, G., and Braun, R.E. (2006). Pathway to totipotency: lessons from germ cells. *Cell* 127, 891–904. <https://doi.org/10.1016/j.cell.2006.11.016>.
2. Spradling, A., Fuller, M.T., Braun, R.E., and Yoshida, S. (2011). Germline stem cells. *Cold Spring Harb. Perspect. Biol.* 3, a002642. <https://doi.org/10.1101/cshperspect.a002642>.
3. Cinalli, R.M., Rangan, P., and Lehmann, R. (2008). Germ cells are forever. *Cell* 132, 559–562. <https://doi.org/10.1016/j.cell.2008.02.003>.
4. Gilboa, L., and Lehmann, R. (2004). Repression of primordial germ cell differentiation parallels germ line stem cell maintenance. *Curr. Biol.* 14, 981–986. <https://doi.org/10.1016/j.cub.2004.05.049>.
5. Lesch, B.J., and Page, D.C. (2012). Genetics of germ cell development. *Nat. Rev. Genet.* 13, 781–794. <https://doi.org/10.1038/nrg3294>.
6. Reik, W., and Surani, M.A. (2015). Germline and pluripotent stem cells. *Cold Spring Harb. Perspect. Biol.* 7, a019422. <https://doi.org/10.1101/cshperspect.a019422>.
7. Lehmann, R. (2012). Germline stem cells: origin and destiny. *Cell Stem Cell* 10, 729–739. <https://doi.org/10.1016/j.stem.2012.05.016>.
8. Yuan, H., and Yamashita, Y.M. (2010). Germline stem cells: stems of the next generation. *Curr. Opin. Cell Biol.* 22, 730–736. <https://doi.org/10.1016/j.ceb.2010.08.013>.
9. Xie, T., and Spradling, A.C. (2000). A niche maintaining germ line stem cells in the *Drosophila* ovary. *Science* 290, 328–330. <https://doi.org/10.1126/science.290.5490.328>.
10. Chen, D., and McKearin, D.M. (2003). A discrete transcriptional silencer in the *bam* gene determines asymmetric division of the *Drosophila* germline stem cell. *Development* 130, 1159–1170. <https://doi.org/10.1242/dev.00325>.
11. Chen, D., and McKearin, D. (2003). Dpp signaling silences *bam* transcription directly to establish asymmetric divisions of germline stem cells. *Curr. Biol.* 13, 1786–1791. <https://doi.org/10.1016/j.cub.2003.09.033>.
12. Xie, T. (2013). Control of germline stem cell self-renewal and differentiation in the *Drosophila* ovary: concerted actions of niche signals and intrinsic factors. *Wiley Interdiscip. Rev. Dev. Biol.* 2, 261–273. <https://doi.org/10.1002/wdev.60>.
13. Huynh, J.-R., and St Johnston, D. (2004). The origin of asymmetry: early polarisation of the *Drosophila* germline cyst and oocyte. *Curr. Biol.* 14, R438–R449. <https://doi.org/10.1016/j.cub.2004.05.040>.
14. Navarro, C., Puthalakath, H., Adams, J.M., Strasser, A., and Lehmann, R. (2004). Egalitarian binds dynein light chain to establish oocyte polarity and maintain oocyte fate. *Nat. Cell Biol.* 6, 427–435. <https://doi.org/10.1038/ncb1122>.
15. Mach, J.M., and Lehmann, R. (1997). An Egalitarian-BicaudalD complex is essential for oocyte specification and axis determination in *Drosophila*. *Genes Dev.* 11, 423–435. <https://doi.org/10.1101/gad.11.4.423>.

Developmental Cell

Article



16. Blatt, P., Wong-Deyrup, S.W., McCarthy, A., Breznak, S., Hurton, M.D., Upadhyay, M., Bennink, B., Camacho, J., Lee, M.T., and Rangan, P. (2021). RNA degradation is required for the germ-cell to maternal transition in *Drosophila*. *Curr. Biol.* 31, 2984–2994.e7. <https://doi.org/10.1016/j.cub.2021.04.052>.
17. Flora, P., McCarthy, A., Upadhyay, M., and Rangan, P. (2017). Role of chromatin modifications in *Drosophila* germline stem cell differentiation. *Results Probl. Cell Differ.* 59, 1–30. https://doi.org/10.1007/978-3-319-44820-6_1.
18. McKearin, D., and Ohlstein, B. (1995). A role for the *Drosophila* Bag-of-marbles protein in the differentiation of cystoblasts from germline stem cells. *Development* 121, 2937–2947. <https://doi.org/10.1242/dev.121.9.2937>.
19. McKearin, D.M., and Spradling, A.C. (1990). bag-of-marbles: a *Drosophila* gene required to initiate both male and female gametogenesis. *Genes Dev.* 4, 2242–2251. <https://doi.org/10.1101/gad.4.12b.2242>.
20. Carreira-Rosario, A., Bhargava, V., Hillebrand, J., Kollipara, R.K., Ramaswami, M., and Buszczak, M. (2016). Repression of pumilio protein expression by Rbfox1 promotes germ cell differentiation. *Dev. Cell* 36, 562–571. <https://doi.org/10.1016/j.devcel.2016.02.010>.
21. Breznak, S.M., Peng, Y., Deng, L., Kotb, N.M., Flamholz, Z., Rapisarda, I.T., Martin, E.T., LaBarge, K.A., Fabris, D., Gavis, E.R., and Rangan, P. (2023). H/ACA snRNP-dependent ribosome biogenesis regulates translation of polyglutamine proteins. *Sci. Adv.* 9, eade5492. <https://doi.org/10.1126/sciadv.ade5492>.
22. McCarthy, A., Sarkar, K., Martin, E.T., Upadhyay, M., Jang, S., Williams, N.D., Forni, P.E., Buszczak, M., and Rangan, P. (2022). Msl3 promotes germline stem cell differentiation in female *Drosophila*. *Development* 149, dev199625. <https://doi.org/10.1242/dev.199625>.
23. Ables, E.T. (2015). *Drosophila* oocytes as a model for understanding meiosis: an educational primer to accompany “corolla is a novel protein that contributes to the architecture of the synaptonemal complex of *Drosophila*”. *Genetics* 199, 17–23. <https://doi.org/10.1534/genetics.114.167940>.
24. Cahoon, C.K., and Hawley, R.S. (2016). Regulating the construction and demolition of the synaptonemal complex. *Nat. Struct. Mol. Biol.* 23, 369–377. <https://doi.org/10.1038/nsmb.3208>.
25. Hughes, S.E., Miller, D.E., Miller, A.L., and Hawley, R.S. (2018). Female meiosis: synapsis, recombination, and segregation in *Drosophila melanogaster*. *Genetics* 208, 875–908. <https://doi.org/10.1534/genetics.117.300081>.
26. Orr-Weaver, T.L. (1995). Meiosis in *Drosophila*: seeing is believing. *Proc. Natl. Acad. Sci. USA* 92, 10443–10449. <https://doi.org/10.1073/pnas.92.23.10443>.
27. Page, S.L., and Hawley, R.S. (2001). c(3)G encodes a *Drosophila* synaptonemal complex protein. *Genes Dev.* 15, 3130–3143. <https://doi.org/10.1101/gad.935001>.
28. Clough, E., Tedeschi, T., and Hazelrigg, T. (2014). Epigenetic regulation of oogenesis and germ stem cell maintenance by the *Drosophila* histone methyltransferase Eggless/dSetDB1. *Dev. Biol.* 388, 181–191. <https://doi.org/10.1016/j.ydbio.2014.01.014>.
29. Rangan, P., Malone, C.D., Navarro, C., Newbold, S.P., Hayes, P.S., Sachidanandam, R., Hannon, G.J., and Lehmann, R. (2011). piRNA production requires heterochromatin formation in *Drosophila*. *Curr. Biol.* 21, 1373–1379. <https://doi.org/10.1016/j.cub.2011.06.057>.
30. Yoon, J., Lee, K.-S., Park, J.-S., Yu, K., Paik, S.-G., and Kang, Y.-K. (2008). dSETDB1 and SU(VAR)3-9 sequentially function during germline-stem cell differentiation in *Drosophila melanogaster*. *PLoS One* 3, e2234. <https://doi.org/10.1371/journal.pone.0002234>.
31. Clough, E., Moon, W., Wang, S., Smith, K., and Hazelrigg, T. (2007). Histone methylation is required for oogenesis in *Drosophila*. *Development* 134, 157–165. <https://doi.org/10.1242/dev.02698>.
32. Koch, C.M., Honemann-Capito, M., Egger-Adam, D., and Wodarz, A. (2009). Windei, the *Drosophila* homolog of mAM/MCAF1, is an essential cofactor of the H3K9 methyl transferase dSETDB1/Eggless in germ line development. *PLoS Genet.* 5, e1000644. <https://doi.org/10.1371/journal.pgen.1000644>.
33. Osumi, K., Sato, K., Murano, K., Siomi, H., and Siomi, M.C. (2019). Essential roles of Windei and nuclear monoubiquitination of Eggless/SETDB1 in transposon silencing. *EMBO Rep.* 20, e48296. <https://doi.org/10.15252/embr.201948296>.
34. Smolko, A.E., Shapiro-Kulnane, L., and Salz, H.K. (2018). The H3K9 methyltransferase SETDB1 maintains female identity in *Drosophila* germ cells. *Nat. Commun.* 9, 4155. <https://doi.org/10.1038/s41467-018-06697-x>.
35. Czech, B., Munafò, M., Ciabrelli, F., Eastwood, E.L., Fabry, M.H., Kneuss, E., and Hannon, G.J. (2018). piRNA-guided genome defense: from biogenesis to silencing. *Annu. Rev. Genet.* 52, 131–157. <https://doi.org/10.1146/annurev-genet-120417-031441>.
36. Malone, C.D., Brennecke, J., Dus, M., Stark, A., McCombie, W.R., Sachidanandam, R., and Hannon, G.J. (2009). Specialized piRNA pathways act in germline and somatic tissues of the *Drosophila* ovary. *Cell* 137, 522–535. <https://doi.org/10.1016/j.cell.2009.03.040>.
37. Smolko, A.E., Shapiro-Kulnane, L., and Salz, H.K. (2020). An autoregulatory switch in sex-specific phf7 transcription causes loss of sexual identity and tumors in the *Drosophila* female germline. *Development* 147, dev192856. <https://doi.org/10.1242/dev.192856>.
38. Jevitt, A., Chatterjee, D., Xie, G., Wang, X.-F., Ottwell, T., Huang, Y.-C., and Deng, W.-M. (2020). A single-cell atlas of adult *Drosophila* ovary identifies transcriptional programs and somatic cell lineage regulating oogenesis. *PLoS Biol.* 18, e3000538. <https://doi.org/10.1371/journal.pbio.3000538>.
39. Seum, C., Reo, E., Peng, H., Rauscher, F.J., III, Spierer, P., and Bontron, S. (2007). *Drosophila* SETDB1 is required for chromosome 4 silencing. *PLoS Genet.* 3, e76. <https://doi.org/10.1371/journal.pgen.0030076>.
40. Lasko, P.F., and Ashburner, M. (1988). The product of the *Drosophila* gene *vasa* is very similar to eukaryotic initiation factor-4A. *Nature* 335, 611–617. <https://doi.org/10.1038/335611a0>.
41. Zaccai, M., and Lipschitz, H.D. (1996). Differential distributions of two adducin-like protein isoforms in the *Drosophila* ovary and early embryo. *Zygote* 4, 159–166. <https://doi.org/10.1017/s096719940000304x>.
42. Chou, T.B., and Perrimon, N. (1996). The autosomal FLP-Dfs technique for generating germline mosaics in *Drosophila melanogaster*. *Genetics* 144, 1673–1679. <https://doi.org/10.1093/genetics/144.4.1673>.
43. Gerbasi, V.R., Preall, J.B., Golden, D.E., Powell, D.W., Cummins, T.D., and Sontheimer, E.J. (2011). Blanks, a nuclear siRNA/dsRNA-binding complex component, is required for *Drosophila* spermiogenesis. *Proc. Natl. Acad. Sci. USA* 108, 3204–3209. <https://doi.org/10.1073/pnas.1009781108>.
44. Ahmad, K. (2018). CUT&RUN with *Drosophila* tissues V.1. <https://doi.org/10.17504/protocols.io.umfeu3n>.
45. Skene, P.J., and Henikoff, S. (2017). An efficient targeted nuclease strategy for high-resolution mapping of DNA binding sites. *eLife* 6, e21856. <https://doi.org/10.7554/eLife.21856>.
46. Devlin, R.H., Bingham, B., and Wakimoto, B.T. (1990). The organization and expression of the light gene, a heterochromatic gene of *Drosophila melanogaster*. *Genetics* 125, 129–140. <https://doi.org/10.1093/genetics/125.1.129>.
47. Schwartz, Y.B., and Cavalli, G. (2017). Three-dimensional genome organization and function in *Drosophila*. *Genetics* 205, 5–24. <https://doi.org/10.1534/genetics.115.185132>.
48. Schubert, H.L., Blumenthal, R.M., and Cheng, X. (2003). Many paths to methyltransfer: a chronicle of convergence. *Trends Biochem. Sci.* 28, 329–335. [https://doi.org/10.1016/S0968-0004\(03\)00090-2](https://doi.org/10.1016/S0968-0004(03)00090-2).
49. Yeates, T.O. (2002). Structures of SET domain proteins. *Cell* 111, 5–7. [https://doi.org/10.1016/S0092-8674\(02\)01010-3](https://doi.org/10.1016/S0092-8674(02)01010-3).
50. Wilson, J.R., Jing, C., Walker, P.A., Martin, S.R., Howell, S.A., Blackburn, G.M., Gamblin, S.J., and Xiao, B. (2002). Crystal structure and functional analysis of the histone methyltransferase SET7/9. *Cell* 111, 105–115. [https://doi.org/10.1016/S0092-8674\(02\)00964-9](https://doi.org/10.1016/S0092-8674(02)00964-9).

51. Andersen, P.R., Tirian, L., Vunjak, M., and Brennecke, J. (2017). A heterochromatin-dependent transcription machinery drives piRNA expression. *Nature* 549, 54–59. <https://doi.org/10.1038/nature23482>.
52. Sienski, G., Döneras, D., and Brennecke, J. (2012). Transcriptional silencing of transposons by Piwi and Maelstrom and its impact on chromatin state and gene expression. *Cell* 151, 964–980. <https://doi.org/10.1016/j.cell.2012.10.040>.
53. Upadhyay, M., Martino Cortez, Y., Wong-Deyrup, S., Tavares, L., Schowalter, S., Flora, P., Hill, C., Nasrallah, M.A., Chittur, S., and Rangan, P. (2016). Transposon dysregulation modulates dWnt4 signaling to control germline stem cell differentiation in *Drosophila*. *PLoS Genet.* 12, e1005918. <https://doi.org/10.1371/journal.pgen.1005918>.
54. Chen, Y., Pane, A., and Schüpbach, T. (2007). *cutoff* and *aubergine* mutations result in retrotransposon upregulation and checkpoint activation in *Drosophila*. *Curr. Biol.* 17, 637–642. <https://doi.org/10.1016/j.cub.2007.02.027>.
55. Wilson, J.E., Connell, J.E., and Macdonald, P.M. (1996). *aubergine* enhances *oskar* translation in the *Drosophila* ovary. *Development* 122, 1631–1639. <https://doi.org/10.1242/dev.122.5.1631>.
56. Capelson, M., Doucet, C., and Hetzer, M.W. (2010). Nuclear pore complexes: guardians of the nuclear genome. *Cold Spring Harb. Symp. Quant. Biol.* 75, 585–597. <https://doi.org/10.1101/sqb.2010.75.059>.
57. Doucet, C.M., and Hetzer, M.W. (2010). Nuclear pore biogenesis into an intact nuclear envelope. *Chromosoma* 119, 469–477. <https://doi.org/10.1007/s00412-010-0289-2>.
58. Gozalo, A., and Capelson, M. (2016). A new path through the nuclear pore. *Cell* 167, 1159–1160. <https://doi.org/10.1016/j.cell.2016.11.011>.
59. Capelson, M., and Hetzer, M.W. (2009). The role of nuclear pores in gene regulation, development and disease. *EMBO Rep.* 10, 697–705. <https://doi.org/10.1038/embor.2009.147>.
60. Hou, C., and Corces, V.G. (2010). Nups take leave of the nuclear envelope to regulate transcription. *Cell* 140, 306–308. <https://doi.org/10.1016/j.cell.2010.01.036>.
61. Iglesias, N., Paulo, J.A., Tatarakis, A., Wang, X., Edwards, A.L., Bhanu, N.V., Garcia, B.A., Haas, W., Gygi, S.P., and Moazed, D. (2020). Native chromatin proteomics reveals a role for specific nucleoporins in heterochromatin organization and maintenance. *Mol. Cell* 77, 51–66.e8. <https://doi.org/10.1016/j.molcel.2019.10.018>.
62. Colozza, G., Montembault, E., Quénérch'du, E., Riparbelli, M.G., D'Avino, P.P., and Callaini, G. (2011). *Drosophila* nucleoporin Nup154 controls cell viability, proliferation and nuclear accumulation of Mad transcription factor. *Tissue Cell* 43, 254–261. <https://doi.org/10.1016/j.tice.2011.05.001>.
63. Gigliotti, S., Callaini, G., Andone, S., Riparbelli, M.G., Pernas-Alonso, R., Hoffmann, G., Graziani, F., and Malva, C. (1998). *Nup154*, a new *Drosophila* gene essential for male and female gametogenesis is related to the *Nup155* vertebrate nucleoporin gene. *J. Cell Biol.* 142, 1195–1207. <https://doi.org/10.1083/jcb.142.5.1195>.
64. Grimaldi, M.R., Cozzolino, L., Malva, C., Graziani, F., and Gigliotti, S. (2007). *nup154* genetically interacts with *cup* and plays a cell-type-specific function during *Drosophila melanogaster* egg-chamber development. *Genetics* 175, 1751–1759. <https://doi.org/10.1534/genetics.106.062844>.
65. Katsani, K.R., Kares, R.E., Dostatni, N., and Doye, V. (2008). In vivo dynamics of *Drosophila* nuclear envelope components. *Mol. Biol. Cell* 19, 3652–3666. <https://doi.org/10.1091/mbc.e07-11-1162>.
66. Davis, L.I., and Blobel, G. (1987). Nuclear pore complex contains a family of glycoproteins that includes p62: glycosylation through a previously unidentified cellular pathway. *Proc. Natl. Acad. Sci. USA* 84, 7552–7556. <https://doi.org/10.1073/pnas.84.21.7552>.
67. Weiler, K.S., and Wakimoto, B.T. (1995). Heterochromatin and gene expression in *Drosophila*. *Annu. Rev. Genet.* 29, 577–605. <https://doi.org/10.1146/annurev.ge.29.120195.003045>.
68. Van de Vosse, D.W., Wan, Y., Lapetina, D.L., Chen, W.-M., Chiang, J.-H., Aitchison, J.D., and Wozniak, R.W. (2013). A role for the nucleoporin Nup170p in chromatin structure and gene silencing. *Cell* 152, 969–983. <https://doi.org/10.1016/j.cell.2013.01.049>.
69. Van de Vosse, D.W., Wan, Y., Wozniak, R.W., and Aitchison, J.D. (2011). Role of the nuclear envelope in genome organization and gene expression. *Wiley Interdiscip. Rev. Syst. Biol. Med.* 3, 147–166. <https://doi.org/10.1002/wsbm.101>.
70. Beliveau, B.J., Joyce, E.F., Apostolopoulos, N., Yilmaz, F., Fonseka, C.Y., McCole, R.B., Chang, Y., Li, J.B., Senaratne, T.N., Williams, B.R., et al. (2012). Versatile design and synthesis platform for visualizing genomes with Oligopaint FISH probes. *Proc. Natl. Acad. Sci. USA* 109, 21301–21306. <https://doi.org/10.1073/pnas.1213818110>.
71. Nguyen, S.C., and Joyce, E.F. (2019). Programmable chromosome painting with Oligopaints. *Methods Mol. Biol.* 2038, 167–180. https://doi.org/10.1007/978-1-4939-9674-2_11.
72. Park, D.S., Nguyen, S.C., Isenhart, R., Shah, P.P., Kim, W., Barnett, R.J., Chandra, A., Luppin, J.M., Harke, J., Wai, M., et al. (2022). High-throughput Oligopaint screen identifies druggable regulators of genome folding. Preprint at bioRxiv. <https://doi.org/10.1101/2022.04.08.487672>.
73. DeLuca, S.Z., Ghildiyal, M., Pang, L.-Y., and Spradling, A.C. (2020). Differentiating *Drosophila* female germ cells initiate Polycomb silencing by regulating PRC2-interacting proteins. *eLife* 9, e56922. <https://doi.org/10.7554/eLife.56922>.
74. Coleman, R.T., and Struhl, G. (2017). Causal role for inheritance of H3K27me3 in maintaining the OFF state of a *Drosophila* HOX gene. *Science* 356, eaai8236. <https://doi.org/10.1126/science.aai8236>.
75. Calvi, B.R., Lilly, M.A., and Spradling, A.C. (1998). Cell cycle control of chorion gene amplification. *Genes Dev.* 12, 734–744. <https://doi.org/10.1101/gad.12.5.734>.
76. Kugler, J.-M., and Lasko, P. (2009). Localization, anchoring and translational control of *oskar*, *gurken*, *bicoid* and *nanos* mRNA during *Drosophila* oogenesis. *Fly* 3, 15–28. <https://doi.org/10.4161/fly.3.1.7751>.
77. Teifer, W.H. (1975). Development and physiology of the oocyte-nurse cell syncytium. *Adv. Insect Physiol.* 11, 223–319. [https://doi.org/10.1016/S0065-2806\(08\)60164-2](https://doi.org/10.1016/S0065-2806(08)60164-2).
78. Tsusaka, T., Shimura, C., and Shinkai, Y. (2019). ATF7IP regulates SETDB1 nuclear localization and increases its ubiquitination. *EMBO Rep.* 20, e48297. <https://doi.org/10.1525/embr.201948297>.
79. Eymery, A., Liu, Z., Ozonov, E.A., Stadler, M.B., and Peters, A.H.F.M. (2016). The methyltransferase *Setdb1* is essential for meiosis and mitosis in mouse oocytes and early embryos. *Development* 143, 2767–2779. <https://doi.org/10.1242/dev.132746>.
80. Duan, T., Green, N., Tootle, T.L., and Geyer, P.K. (2020). Nuclear architecture as an intrinsic regulator of *Drosophila* female germline stem cell maintenance. *Curr. Opin. Insect Sci.* 37, 30–38. <https://doi.org/10.1016/j.cois.2019.11.007>.
81. Capelson, M., Liang, Y., Schulte, R., Mair, W., Wagner, U., and Hetzer, M.W. (2010). Chromatin-bound nuclear pore components regulate gene expression in higher eukaryotes. *Cell* 140, 372–383. <https://doi.org/10.1016/j.cell.2009.12.054>.
82. Holla, S., Dhakshnamoorthy, J., Folco, H.D., Balachandran, V., Xiao, H., Sun, L.-L., Wheeler, D., Zofall, M., and Grewal, S.I.S. (2020). Positioning heterochromatin at the nuclear periphery suppresses histone turnover to promote epigenetic inheritance. *Cell* 180, 150–164.e15. <https://doi.org/10.1016/j.cell.2019.12.004>.
83. Brickner, D.G., Randise-Hinchliff, C., Lebrun Corbin, M., Liang, J.M., Kim, S., Sump, B., D'Urso, A., Kim, S.H., Satomura, A., Schmit, H., et al. (2019). The role of transcription factors and nuclear pore proteins in controlling the spatial organization of the yeast genome. *Dev. Cell* 49, 936–947.e4. <https://doi.org/10.1016/j.devcel.2019.05.023>.
84. McCloskey, A., Ibarra, A., and Hetzer, M.W. (2018). Tpr regulates the total number of nuclear pore complexes per cell nucleus. *Genes Dev.* 32, 1321–1331. <https://doi.org/10.1101/gad.315523.118>.
85. Schindelin, J., Arganda-Carreras, I., Frise, E., Kaynig, V., Longair, M., Pietzsch, T., Preibisch, S., Rueden, C., Saalfeld, S., Schmid, B., et al.

Developmental Cell

Article



- (2012). Fiji: an open-source platform for biological-image analysis. *Nat. Methods* 9, 676–682. <https://doi.org/10.1038/nmeth.2019>.
86. Kim, D., Langmead, B., and Salzberg, S.L. (2015). HISAT: a fast spliced aligner with low memory requirements. *Nat. Methods* 12, 357–360. <https://doi.org/10.1038/nmeth.3317>.
87. Love, M.I., Huber, W., and Anders, S. (2014). Moderated estimation of fold change and dispersion for RNA-seq data with DESeq2. *Genome Biol.* 15, 550. <https://doi.org/10.1186/s13059-014-0550-8>.
88. Liao, Y., Smyth, G.K., and Shi, W. (2014). featureCounts: an efficient general purpose program for assigning sequence reads to genomic features. *Bioinformatics* 30, 923–930. <https://doi.org/10.1093/bioinformatics/btt656>.
89. Wickham, H. (2016). Data analysis. In *Use R! ggplot2: Elegant Graphics for Data Analysis*, H. Wickham, ed. (Springer International Publishing), pp. 189–201. https://doi.org/10.1007/978-3-319-24277-4_9.
90. Babraham Bioinformatics. FastQC: a quality control tool for high throughput sequence data. <https://www.bioinformatics.babraham.ac.uk/projects/fastqc/>.
91. Ramírez, F., Ryan, D.P., Grüning, B., Bhardwaj, V., Kilpert, F., Richter, A.S., Heyne, S., Dündar, F., and Manke, T. (2016). deepTools2: a next generation web server for deep-sequencing data analysis. *Nucleic Acids Res.* 44, W160–W165. <https://doi.org/10.1093/nar/gkw257>.
92. Flora, P., Wong-Deyrup, S.W., Martin, E.T., Palumbo, R.J., Nasrallah, M., Oligney, A., Blatt, P., Patel, D., Fuchs, G., and Rangan, P. (2018). Sequential regulation of maternal mRNAs through a conserved *cis*-acting element in their 3' UTRs. *Cell Rep.* 25, 3828–3843.e9. <https://doi.org/10.1016/j.celrep.2018.12.007>.
93. Mi, H., Huang, X., Muruganujan, A., Tang, H., Mills, C., Kang, D., and Thomas, P.D. (2017). PANTHER version 11: expanded annotation data from Gene Ontology and Reactome pathways, and data analysis tool enhancements. *Nucleic Acids Res.* 45, D183–D189. <https://doi.org/10.1093/nar/gkw1138>.
94. Amemiya, H.M., Kundaje, A., and Boyle, A.P. (2019). The ENCODE blacklist: identification of problematic regions of the genome. *Sci. Rep.* 9, 9354. <https://doi.org/10.1038/s41598-019-45839-z>.
95. Heinz, S., Benner, C., Spann, N., Bertolino, E., Lin, Y.C., Laslo, P., Cheng, J.X., Murre, C., Singh, H., and Glass, C.K. (2010). Simple combinations of lineage-determining transcription factors prime *cis*-regulatory elements required for macrophage and B cell identities. *Mol. Cell* 38, 576–589. <https://doi.org/10.1016/j.molcel.2010.05.004>.
96. Valm, A.M., Cohen, S., Legant, W.R., Melunis, J., Hershberg, U., Wait, E., Cohen, A.R., Davidson, M.W., Betzig, E., and Lippincott-Schwartz, J. (2017). Applying systems-level spectral imaging and analysis to reveal the organelle interactome. *Nature* 546, 162–167. <https://doi.org/10.1038/nature22369>.

STAR★METHODS

KEY RESOURCES TABLE

REAGENT or RESOURCE	SOURCE	IDENTIFIER
Antibodies		
Rabbit polyclonal anti-GFP	Abcam	ab6556
Mouse monoclonal anti-GFP	Sigma	G6539
Rat monoclonal anti-HA high affinity Mouse anti-1B1	Developmental Studies Hybridoma Bank	Antibody Registry ID: 528070
Rabbit polyclonal anti-Vasa	Rangan lab	N/A
Chicken polyclonal anti-Vasa	Rangan lab	N/A
Rabbit polyclonal anti-Blanks	gift from Sontheimer lab	N/A
Rabbit polyclonal anti-Egalitarian	gift from Lehmann lab	N/A
Rabbit polyclonal anti-H3K9me3	Active Motif	39062
Mouse monoclonal anti-H3K9me3	Active Motif	61013
Mouse monoclonal anti-H3K27me3	Abcam	Ab6002
Mouse monoclonal anti-NPC (mAb414)	BioLegend	902902
Mouse monoclonal anti-LamC	Developmental Studies Hybridoma Bank	Antibody Registry ID: AB_528339
Anti-rabbit Alexa 488	Jackson ImmunoResearch Labs	code: 711-546-152
Anti-mouse Alexa 488	Jackson ImmunoResearch Labs	code: 715-546-150
Anti-mouse Cy3	Jackson ImmunoResearch Labs	code: 715-166-150
Anti-rabbit Cy3	Jackson ImmunoResearch Labs	code: 711-166-152
Anti-rat Cy3	Jackson ImmunoResearch Labs	code: 712-166-150
Anti-chicken Alexa 647	Jackson ImmunoResearch Labs	code: 703-606-155
Chemicals, peptides, and recombinant proteins		
Formaldehyde (Methanol Free), 10% Ultrapure	Polysciences Inc.	#04018-1
Donkey Serum	Sigma-Aldrich	SKU: D9663
Vectashield Antifade Mounting Medium with DAPI	Vector Laboratories	#H-1200
Triton X-100 detergent	VWR	#97062-208
Nonidet P-40 (NP-40) substitute	IBI Scientific	#9016-45-9
Tween-20 detergent	VWR	#97062-332
TRIzol	Invitrogen	#15596026
Complete, EDTA-free Protease Inhibitor Cocktail Pill	Sigma-Aldrich	SKU: 5892953001
OmniPur® Formamide, Deionized	Calbiochem	4650
Pierce™ 16% Formaldehyde (w/v), Methanol-free	Thermo Fisher Scientific	28906
10X PBS buffer, pH7.4	Invitrogen	AM9625
UltraPure 20X SSC buffer	Invitrogen	15557-044
BSA	VWR	E588-100G
SuperScript II	Invitrogen	18064022
RNase A	Thermo scientific	EN0531
Proteinase K	Thermo scientific	EO0491
EDTA	Millipore Sigma	CAS no. 6381-92-6
99% Spermidine	Beantown Chemical	215885-1G
HEPES	Thermo Fisher Scientific	CAS no. 7365-45-9
Polyethylene Glycol 8000	Millipore Sigma	CAS no. 25322-68-3

(Continued on next page)

Developmental Cell

Article



Continued

REAGENT or RESOURCE	SOURCE	IDENTIFIER
Critical commercial assays		
TURBO DNA-free Kit	Life Technologies	AM1907
NEXTflex Rapid Illumina DNA-Seq Library Prep Kit	BioO Scientific	NOVA-5138-11
NEBNext® Ultra II DNA Library Prep Kit for Illumina	New England Biolabs	NEB #E7645, E7103
Stellaris® RNA FISH Hybridization Buffer	LGC Biosearch Technologies	SMF-HB1-10
SYBR Green Master Mix	Applied Biosystems	4367659
Deposited data		
RNA seq Data	this study	GSE186982
CUT&RUN Data	this study	GSE186982
Experimental models: Organisms/strains		
<i>UAS-Dcr2;nosGAL4</i>	Bloomington Drosophila Stock Center	25751
<i>nosGAL4;MKRS/TM6</i>	Bloomington Drosophila Stock Center	4442
<i>UAS-EGFP</i>	Bloomington Drosophila Stock Center	5431
<i>If/CyO;nosGAL4</i>	Lehmann lab	N/A
<i>SETDB1</i> RNAi	Perrimon lab; Bloomington Drosophila Stock Center	N/A; 24106
<i>Wde</i> RNAi	Bloomington Drosophila Stock Center; Vienna Drosophila Resource Center	33339; V105719
<i>Nup154</i> RNAi	Bloomington Drosophila Stock Center	34710
<i>Nup62</i> RNAi	Bloomington Drosophila Stock Center	35695
<i>Nup107</i> RNAi	Bloomington Drosophila Stock Center	43189
<i>Nup205</i> RNAi	Vienna Drosophila Resource Center	V38608
<i>FRT42B, SETDB1</i> ¹⁴⁷³	Wodarz lab	N/A
<i>FRT42B, wde</i> ^{TD63}	Wodarz lab	N/A
<i>dSETDB1-HA</i>	Bontron Lab	N/A
<i>RpS19b::GFP</i>	Busczak Lab	N/A
<i>mRFP-Nup107</i>	Bloomington Drosophila Stock Center	35516
<i>UAS-SETDB1</i> ^{RNAi-res_WT-GFP}	this study	N/A
<i>UAS-SETDB1</i> ^{RNAi-res_Y-A-GFP}	this study	N/A
Oligonucleotides		
Primers	this study (Table S3)	N/A
Stellaris Probe Against <i>blanks</i> labeled with CALFluor590	LGC Biosearch Technologies	CDS
Stellaris Probe Against <i>RpS19b</i> labeled with CALFluor590	LGC Biosearch Technologies	CDS
DNA probes against <i>RpS19b</i> gene locus	Gift from Joyce lab	N/A
Recombinant DNA		
Gateway Destination Vector	Drosophila Genomics Resource Center	Gateway 1 Collection
Plasmid: pPGW		
Software and algorithms		
ImageJ	Schindelin et al. ⁸⁵	https://imagej.nih.gov/ij/
HISAT2	Kim et al. ⁸⁶	https://ccb.jhu.edu/software/hisat2/index.shtml
DESeq2	Love et al. ⁸⁷	http://www.bioconductor.org/packages/release/bioc/html/DESeq2.html
featureCounts	Liao et al. ⁸⁸	http://bioinf.wehi.edu.au/featureCounts/
ggplot2	Wickham ⁸⁹	https://cran.r-project.org/web/packages/ggplot2/index.html

(Continued on next page)

Continued

REAGENT or RESOURCE	SOURCE	IDENTIFIER
FastQC	Andrews ⁹⁰	https://www.bioinformatics.babraham.ac.uk/projects/fastqc/
deepTools	Ramírez et al. ⁹¹	https://deeptools.readthedocs.io/en/develop/

RESOURCE AVAILABILITY

Lead contact

Requests for further information and resources and reagents should be directed to and will be fulfilled by the lead contact, Prashanth Rangan (prashanth.rangan@mssm.edu).

Materials availability

All flies generated and used in this study are available on request.

Data and code availability

RNA-seq and CUT&RUN data have been deposited at Gene Expression Omnibus (GEO). Data generated during this study are available at GEO databank under accession number GSE186982.

Any additional information required to reanalyze the data reported in this work paper is available from the [lead contact](#) upon request.

EXPERIMENTAL MODEL AND STUDY PARTICIPANT DETAILS

Husbandry conditions of experimental animals

Flies were grown at 25°C–29°C and dissected between 0–3 days post-eclosion.

Fly food was made using the procedures as previously described (summer/winter mix) and narrow vials (Fisherbrand Drosophila Vials; Fischer Scientific) were filled to approximately 10–12mL.⁹²

Fly lines

The following RNAi stocks were used in this study; if more than one line is listed, then both were quantitated and the first was shown in the main figure: *SETDB1* RNAi (Perrimon lab),²⁹ Bloomington #24106, *wde* RNAi (Bloomington #33339, VDRC #105719), *Nup154* RNAi (Bloomington #34710), *Nup62* RNAi (Bloomington #35695), *Nup107* RNAi (Bloomington #43189), *Nup205* RNAi (VDRC #V38608), *FRT42B*, *SETDB1*¹⁴⁷³ (Wodarz lab), *FRT42B*, *wde*^{TD63} (Wodarz lab). Germ line clones for *SETDB1* and *wde* were generated using a heat shock promoter driven flippase on the X-chromosome.³²

The following tagged lines were used in this study: *dSETDB1-HA* (Bontron lab),³⁹ *RpS19b::GFP* (Buszczak lab,²²) *mRFP-Nup107* (Bloomington #35516), *UAS-EGFP* (Bloomington #5431), *UAS-SETDB1*^{RNAi-res_WT}-*GFP* (This study), *UAS-SETDB1*^{RNAi-res_Y-A}-*GFP* (this study).

The following tissue-specific drivers and double balancer lines were used in this study: *UAS-Dcr2:nosGAL4* (Bloomington #25751), *nosGAL4;MKRS/TM6* (Bloomington #4442), and *If/CyO:nosGAL4* (Lehmann lab).

METHOD DETAILS

UAS-SETDB1-GFP overexpression line construction

We re-coded the sequence targeted by the *SETDB1* RNAi line by making synonymous changes at each codon based on the codon usage table in *Drosophila*. The synonymous changes made the gene resistant to RNAi knockdown but did not alter the amino-acid sequence of *SETDB1*. Using the RNAi resistant line as background we also designed a mutant line where the predicted catalytic Tyrosine residue was re-coded such that the mutant gene codes for Alanine instead. The resulting insert sequence was synthesized by GenScript and cloned into a plasmid we generated that contains *UASp* to drive them in the germline and has GFP to mark the presence of the transgene. We submitted the transgenic constructs to The BestGene Inc (Chino Hills, CA) for injection into *w¹¹¹⁸* flies.

Dissection and Immunostaining

Ovaries were dissected and teased apart with mounting needles in cold PBS and kept on ice. All incubation was done with nutation. Samples were fixed for 10 min in 5% methanol-free formaldehyde. Ovaries were washed in 0.5 mL PBT (1X PBS, 0.5% Triton X-100, 0.3% BSA) 4 times for 5 min each. Primary antibodies in PBT were added and incubated at 4°C nutating overnight. Samples were next washed 3 times for 5 min each in 0.5 mL PBT, and once in 0.5 mL PBT with 2% donkey serum (Sigma) for 15 min. Secondary antibodies were added in PBT with 4% donkey serum and incubated at room temperature for 3–4 h. Samples were washed 3 times

for 10 min each in 0.5 mL of 1X PBST (0.2% Tween 20 in 1x PBS) and incubated in Vectashield with DAPI (Vector Laboratories) for 1 h before mounting.

The following primary antibodies were used: mouse anti-1B1 (1:20; DSHB), rabbit anti-Vasa (1:1,000; Rangan lab), chicken anti-Vasa (1:1,000; Rangan lab),⁵³ rabbit anti-GFP (1:2,000; Abcam, ab6556), rabbit anti-H3K9me3 (1:500; Active Motif, AB_2532132), mouse anti-H3K27me3 (1:500; Abcam, ab6002), rabbit anti-Egl (1:1,000; Lehmann lab), mouse anti-NPC (1:2000; BioLegend, AB_2565026), and rat anti-HA (1:500; Roche, 11 867 423 001). The following secondary antibodies were used: Alexa 488 (Molecular Probes), Cy3 and Cy5 (Jackson Labs) were used at a dilution of 1:500. For each staining, we stained at least five pairs of ovaries and each experiment was repeated three times independently.

Fluorescence imaging

The tissues were visualized, and images were acquired using a Zeiss LSM-710 confocal microscope under 20X, 40X, and 63X oil objective with pinhole set to 1 airy unit. All gain, laser power, and other relevant settings were kept constant for any immunostainings being compared. Image processing was done using Fiji and gain adjustment and cropping was performed in Photoshop CC 2019.

Egg laying assays

Assays were conducted in vials with 3 control or experimental females under testing and 1 wild type control males. Crosses were set up in triplicate for both control and experimental. All flies were 1-day old post-eclosion upon setting up the experiment. Cages were maintained at 29°C and plates were changed daily for counting. Analyses were performed for 5 consecutive days. Number of eggs laid were counted and averaged. Adult flies eclosed were counted from all the vials and averaged.

RNA isolation

Ovaries from flies were dissected in cold 1x PBS. RNA was isolated using TRIzol (Invitrogen, 15596026).^{16,22}

RNA was treated with DNase (TURBO DNA-free Kit, Life Technologies, AM1907), and then run on a 1% agarose gel to check integrity of the RNA.

RNA-seq library preparation and analysis

Libraries were prepared using the Biooscientific kit. To generate mRNA enriched libraries, total RNA was treated with poly(A)tail selection beads (Bioo Scientific Corp., NOVA-512991). Manufacturer's instructions of the NEXTflex Rapid Directional RNA-seq Kit (Bioo Scientific Corp., NOVA-5138-08) were followed, but RNA was fragmented for 13 min. Library quality was assessed with a Fragment Analyzer (5200 Fragment Analyzer System, AATI, Ankeny, IA, USA) following manufacturer's instructions. Single-end mRNA sequencing (75 base pair reads) was performed on biological duplicates from each genotype on an Illumina NextSeq500 by the Center for Functional Genomics (CFG).

After quality assessment, the sequenced reads were aligned to the *Drosophila melanogaster* genome (UCSCdm6) using HISAT2 (version 2.1.0) with the RefSeq-annotated transcripts as a guide.⁸⁶ Differential gene expression was assayed by DeSeq2, using a false discovery rate (FDR) of 0.05, and genes with 2-fold or higher were considered significant. The raw and unprocessed data for RNA-seq generated during this study are available at Gene Expression Omnibus (GEO) databank under accession number: GSE186982 (Token number: wlenykcoldmzfqf). GO term enrichment on differentially expressed genes was performed using Panther.⁹³

Fluorescent *in situ* hybridization

A modified RNA *in situ* hybridization procedure for *Drosophila* ovaries was followed. RNA probes were designed and generated by LGC Biosearch Technologies using Stellaris RNA FISH Probe Designer, with specificity to target base pairs of target mRNAs. Ovaries (three pairs per sample) were dissected in RNase free 1X PBS and fixed in 1 mL of 5% formaldehyde for 10 min. The samples were then permeabilized in 1 mL of Permeabilization Solution (PBST+1% Triton-X) rotating in RT for 1 h. Samples were then washed in the wash buffer for 5 minutes (10% deionized formamide and 10% 20x SSC in RNase-free water). Ovaries were covered and incubated overnight with 1ul of probe in hybridization solution (10% dextran sulfate, 1 mg/mL yeast tRNA, 2 mM RNaseOUT, 0.02 mg/mL BSA, 5x SSC, 10% deionized formamide, and RNase-free water) at 30°C. Samples were then washed twice in 1 mL wash buffer for 30 minutes and mounted in Vectashield.

For DNA *in situ* hybridization, the DNA probes were generated by the Joyce lab at University at Pennsylvania. A modified DNA *in situ* hybridization procedure for *Drosophila* imaginal discs was followed. Ovaries were dissected and teased in 1X PBS and fixed in 800 µL of fixative solution (10% formaldehyde, 1 µL 100% NP-40, 20 µL 10X PBS) for 10 min. The ovaries were quickly washed and permeabilized in PBX (1.5 mL Triton-X in 500 mL 1X PBS) for 30 min. Samples were then incubated overnight with primary antibodies in PBX at 4°C. Ovaries were then washed with 1X PBX and incubated with secondary antibodies in 1X PBX for 2 h at RT. The samples were quickly washed with 2X SSCT (500 µL Tween-20 in 50 mL of 2X SSC). The samples were then subjected to three consecutive washes with 2X SSCT + 20% formamide, 2X SSCT + 40% formamide, 2X SSCT + 50% formamide (vol/vol) for 10 min each at RT. The last wash was repeated twice. Then the ovaries were transferred to a PCR tube in 50% formamide and DNA was pre-denatured at 37°C for 4 h, 92°C for 3 min, and 60°C for 20 min. The formamide solution was then replaced with 36 µL of probe buffer (50% formamide in 2X SSCT + 10% dextran sulfate + 4ul of probe) + 1ul with RNase A. Avoid adding more than 4ul of probe in one reaction mixture. This was followed by overnight incubation (19 hours) at 37°C in the dark with shaking. Next, the samples were washed twice with 50%

formamide-2X SSCT solution at 37°C with shaking for 30 minutes each followed by one 10 min wash in 20% formamide-2X SSCT solution at RT. The ovaries were then mounted in vectashield.

CUT&RUN assay

Ovaries from flies were dissected in ice cold 1x PBS and ovarioles were separated by teasing after dissection with mounting needles. PBS was removed and the samples were permeabilized in 1mL of Permeabilization Solution (PBST+1% Triton-X) rotating in RT for 1 h. Samples were then incubated overnight at 4°C in primary antibody dilutions in freshly prepared BBT+ buffer (PBST + 1% BSA + 0.5 mM Spermidine + 2 mM EDTA + 1 large Roche complete EDTA-free tablets). Primary antibody was replaced with BBT+ buffer and quickly washed twice. Samples were then incubated in ~700 ng/mL of pAG-MNase in BBT+ buffer rotating for 4 h at 25°C. Samples were then quickly washed twice in wash + buffer (20 mM HEPES pH 7.5 + 150 mM NaCl + 0.1% BSA + 0.5 mM Spermidine + 1 large Roche complete EDTA-free tablets in water). Samples were resuspended in 150 µL Wash+C (wash+ + 100 mM CaCl₂) and incubated for 45 minutes on nutator at 4°C. The cleavage reaction was terminated by addition of 150 µL StopR (NaCl final 200 mM + EDTA final 20 mM + 100 µg/mL RNaseA) and incubating the sample at 37C for 30 min. Samples were then centrifuged at 16,000 x g for 5 min and 300 µL of the supernatant was collected for DNA discovery. To the supernatant, 2 µL 10% SDS and 2.5 µL of 20 mg /mL Proteinase K was added and incubated at 50°C for 2 h. Half of this was kept as a backup and half was used in bead cleanup. 20 µL AmpureXP bead slurry and 280 µL MXP buffer (20% PEG8000 + 2.5 M NaCl + 10 mM MgCl₂ in water) was added to the sample and mixed thoroughly followed by 15 min incubation at RT. The beads were separated by magnet and supernatant was discarded. The beads were carefully washed with 80% ethanol for 30 s, while on the magnetic stand and air dried for 2 min. The beads were then resuspended in 10 µL DNase free water.

DNA seq library preparation and analysis

The samples from CUT&RUN assay were used for library preparation using NEBNext Ultra DNA Library Prep Kit for Illumina (E7645, E7103) and adaptor ligated DNA were prepared without size selection.

CUT&RUN data analysis

CUT&RUN libraries were sequenced as paired-end 75bp reads on the Illumina NextSeq 500 at the University at Albany Center for Functional Genomics. FASTQ files were aligned to the dm6 reference genome using HISAT2 (10.1038/s41587-019-0201-4) (-X 10 -I 1000 –no-spliced-alignment, –no-discordant). Mapping statistics and data will be available from Gene Expression Omnibus. Alignment files were sorted and indexed using samtools and were subsequently used to create bigwig files for visualization with deeptools (-binSize 10).⁹¹ Principal-component analysis between samples was performed using the multiBigwigSummary and plotPCA modules from deeptools. Only gene bodies were considered, and problematic genomic regions (blacklist) were removed from the analysis.⁹⁴ Raw read counts of H3K9me3 enrichment across gene bodies was calculated using the HOMER annotateRepeats function and differential enrichment was calculated using DESeq2.⁹⁵ H3K9me3 occupied genes are those with differential enrichment of H3K9me3 compared to IgG matched control conditions using DESeq2.

Quantitative Real Time-PCR (qRT-PCR)

1 µL of cDNA from each genotype was amplified using 5 µL of SYBR green Master Mix, 0.3 µL of 10 µM of each reverse and forward primers in a 10 µL reaction. The thermal cycling conditions consisted of 50°C for 2 min, 95°C for 10 min, 40 cycles at 95°C for 15 s, and 60°C for 60 seconds. The experiments were carried out in technical triplicate and minimum two biological replicates for each sample. To calculate fold change in mRNA levels, comparison was done to rp49 mRNA levels which was used as the control gene. Average of the 2^{ΔΔCt} for the biological replicates was calculated. Error bars were plotted using standard error of the ratios and P-value was determined by Student's t-test.

QUANTIFICATION AND STATISTICAL ANALYSIS

Quantifications of egg chamber area and fluorescent intensity

To quantify antibody staining intensities for GFP, RFP, HA, NPC, LamC, H3K9me3 and H3K27me3 or *in situ* probe fluorescence, images for both control and experimental ovariole were taken using the same confocal settings. Z stacks were obtained for all images. Similar planes in control and experimental were chosen, the area of cells or nuclei positive for the proteins or *in situ*s of interest was outlined and quantified using the ‘measurement’ tool in Fiji (ImageJ). The mean intensity and area of the specified region was obtained. An average of all the ratios (mean/area), for the proteins or *in situ*s of interest, per image was calculated for both control and experimental. Germline intensities were normalized to somatic intensities, if the protein or *in situ* of interest is germline enriched and not expressed in the soma, they were normalized to Vasa.

GFP levels in RpS19b::GFP flies were measured by outlining undifferentiated cells, cysts and egg chambers in germline specific manner and mean GFP intensity was measured. Nuclear HA levels in SETDB1-HA flies were quantified by outlining nucleus of cells pre and post oocyte specification and measuring mean HA intensity of a z stack. Cytoplasmic HA level was measured by quantifying the mean level of HA of a constant cytoplasmic area in multiple cells. HA level was normalized to either DAPI or somatic HA level in the follicle cells. H3K9me3 level was measured by outlining the nucleus and measuring the mean intensity of H3K9me3. It was then normalized to DAPI level. We also measured H3K9me3 intensity using stacks (see below). For the NPC quantification, we outlined

the nuclear envelope based on the DAPI channel and measured the intensity of the NPC (mab414) channel. The NPC level quantified includes protein level at the nuclear envelope and not in the nucleoplasm or cytoplasm. Same was done for quantifying RFP and LamC in germline and somatic cells. Germline RFP/LamC intensity was then normalized to surrounding somatic level.

To measure the area of the germlines of egg chambers, planes in the middle of the egg chamber were chosen for control and experimental ovariole and put into a stack. Next, using the vasa channel the germline of each egg chamber was outlined and area was measured using ‘measurement’ tool in ImageJ.

For all measurements, a minimum of five pairs of ovaries were dissected and a minimum of five independent ovarioles were used for all quantitation. For all quantification, N represents number of ovarioles, which is mentioned in respective figure legends.

GraphPad (Prism) was used for all statistical analysis, details of which can be found in the figure legends. No method was used to determine whether the data met assumptions of the statistical approach. The statistical analysis for the data is found in the figures and figure legends.

Colocalization analysis

Confocal images of control and Nup154-RNAi mutants labeled for RFP-Nup107, H3K9me3, and DAPI were imported into Bitplane Imaris 9.6.2 for 3D reconstruction and colocalization analysis. Colocalization between RFP-Nup107 and H3K9me3 was calculated on a per egg chamber basis using the Surface-surface coloc function of Imaris and an automatic threshold detection and the surface-to-surface coloc function. The number of colocalized voxels was then normalized to the number of H3K9me3 voxels.⁹⁶

Quantification of H3K9me3 mark distance from nuclear periphery

Confocal images of control and *Nup154* GKD mutants, labeled for lamin C and H3K9me3 were imported into Bitplane Imaris 9.6.2 for 3D spatial analysis. Nuclei of interest were isolated and the lamin C label defining the nuclear periphery was used to generate surface objects.

The center of mass for each H3Kme3 puncta was identified using the spots object function in Imaris. The distance of each H3K9me3 spot to the closest lamin C surface boundary was generated and the shortest distance was calculated (spot to surface distance). The mean of the distances of all H3K9me3 spots in a nucleus to the closest laminin surface boundary was calculated for both control and *Nup154* GKD mutants. One-tailed Welch’s t test was used to calculate p-values for significance.